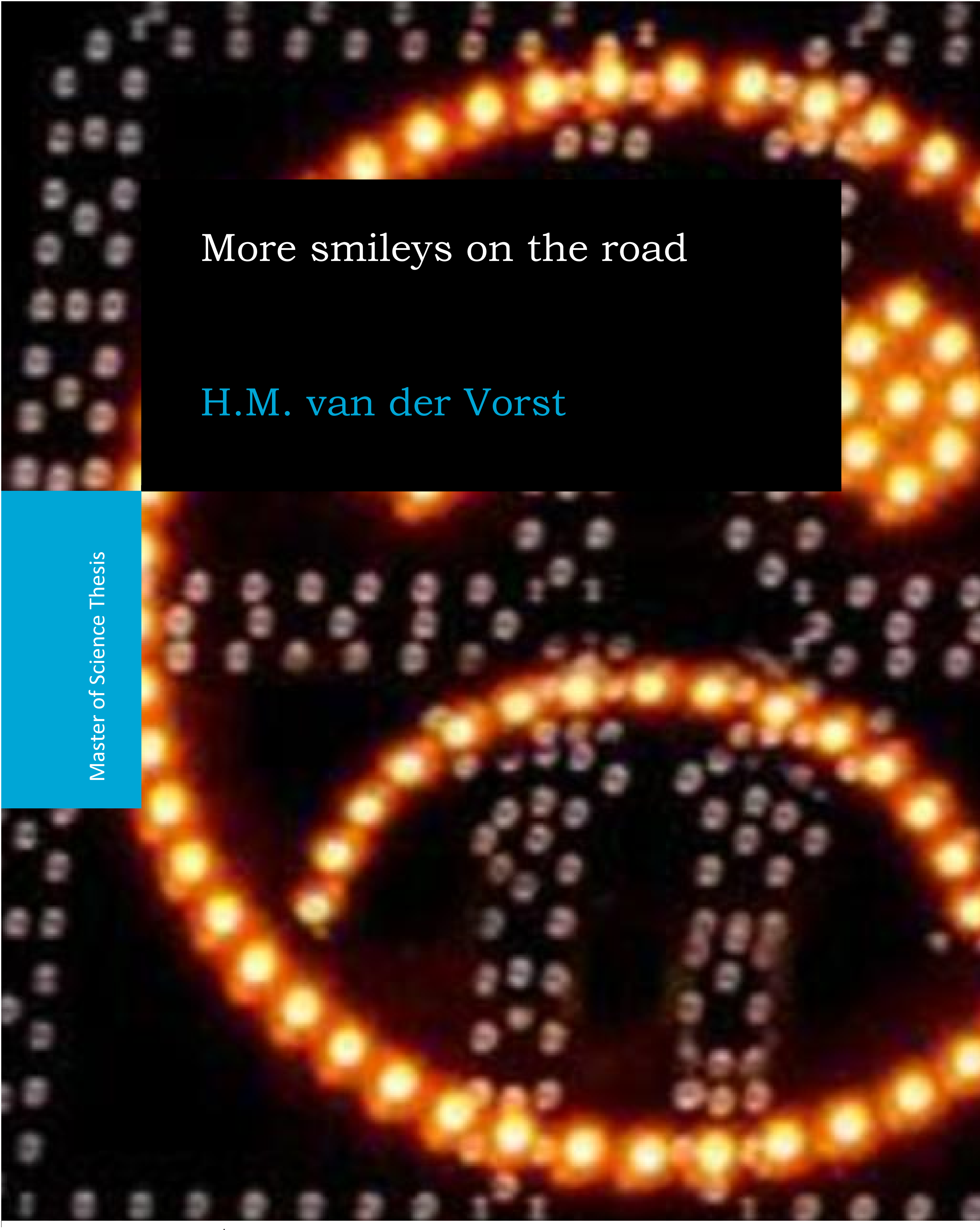

More smileys on the road

H.M. van der Vorst

Master of Science Thesis

Delft University of Technology

Delft Center for Systems and Control

More Smileys on the road

Master of Science Thesis

For the degree of Master of Science in Systems and Control at Delft University of Technology

H.M. van der Vorst

April 21, 2017

Faculty of Mechanical, Maritime and Materials Engineering (3mE) · Delft University of Technology

Abstract

Congestion is one of the big annoyances people experience in their everyday life. Furthermore, congestion has negative effects on both the environment and the economy. In short, it forms a very big problem to society.

This thesis focuses on a specific type of congestion, namely a ‘wide moving jam’. This is typically a short jam that propagates in the opposite direction of the traffic. The short jam usually originates at a ‘weak link’ of any specific road. An example of such a weak link is the location where four lanes become three lanes and people are asked to merge. The general rule is that the outflow of traffic in a wide moving jam is 30% lower than the free capacity of the road. This means that the realized capacity of the road can be much lower than the theoretical capacity. A very well-known example of this in the Netherlands is the freeway route A13-A20-A16 which passes Rotterdam. It has been shown that a large part of the congestion on the A13 is caused by moving jams [Vonk Noordegraaf, 2013]. This route will be the subject of the analysis performed in this thesis.

Often there is a combination of factors that contribute to the formation of a wide moving jam. Speed and density are high but there is another specific reason (or more) at play. In such a situation the state of traffic is not stable and therefore a small disruption can cause a jam. The general strategy in combatting these wide moving jams is to lower the inflow of traffic onto the jam. Algorithms have been developed that are able to detect and dissolve wide moving jams with use of variable speed signs to control traffic flow. However, while this measure is successful in solving a wide moving jam there are side effects. The variable speed sign changes the behaviour of the road users in such a way that congestion will form elsewhere. It has been studied that the impact of the side effects are in the same order of magnitude as the initial problem.

Instead of cutting off the flow to solve the moving jam why not stimulate the flow at the known locations where they originate? In this thesis it is proposed to solve the operational bottleneck that causes a wide moving jam by stimulating vehicles to maintain their speed. At the origin of a wide moving jam a dynamic road sign will be placed that displays your speed with a L if you are driving too

slow and a J if your speed is sufficient. To investigate the effect of stimulating vehicles to increase or maintain their speed, traffic is divided into two groups, a fast group and a slow group. Simulations are done where vehicles from the fast group and the slow groups are mixed. The range of free speed is constant but the compositions of vehicles with high free speed and low free speed is variable.

The simulations show how more uniform free speed results in less congestion in both cases, whether the ratio of fast to low vehicles is close to 100 or 0. The difference is in the level of congestion, when the majority of vehicles are fast the flow discharge rate stays approximately constant. However, when the majority of vehicles is slow, the flow discharge rate is not. As the percentage of fast vehicles is decreased congestion decreases but speed in congestion decreases as well, therefore the critical density decreases.

A smiley traffic sign that encourages vehicles to increase their speed can be used in combatting wide moving jams by reducing the bottleneck and therefore the chance a wide moving jam will form. When speed and density are high a smaller disruption is less likely to cause a wide moving jam. It is difficult to define a critical size for the bottleneck as it depends on the state of traffic. However, it is found that when the percentage of fast vehicles succeeds the percentage of slow vehicles the speed inside the congestion is more stable.

Table of Contents

Acknowledgements

This thesis marks the end of an era which I can best describe by saying it was lengthy and the struggle was real. Often I have felt defeated but never gave up and for this I have to thank my parents and sisters. Their never ending support and faith made me able to do this. In particular Noortje, who I always count on, has helped me to create order in a world full of chaos with her constructive criticism and general fabulousness.

I would like to thank Hans Hellendoorn for his patience, understanding and positive attitude and for being the one thing I will miss.

I am excited to start a new era in my life, feeling blessed with all the things I have learnt inside or outside the university, with all the people I have met and come to love and with pride for what I have accomplished.

1 Introduction

Congestion is one of the big annoyances people experience in their everyday life. In 2011 Dutch drivers wasted 50 hours in traffic, according to a study by INRIX[1]. Furthermore congestion has negative effects on both the environment and the economy. In short, it forms a very big problem to society.

The concept of congestion seems pretty straight-forward: it occurs whenever the capacity of the road is exceeded by the travel demand. When stated like this, an obvious solution for the problem would be to limit the travel demand to the capacity of the road, or to increase the capacity of the road to the demand. Unfortunately, the solution to congestion is a lot less straight-forward than its concept.

The problem is that the capacity of the road is not just a property defined by controllable factors like the speed limit, the length of the road and the number of lanes. There are a lot of different factors contributing to the congestion we experience every day. The six most important disturbances to the capacity of the road are (1) limited physical capacity (bottlenecks) (2) poorly functioning traffic signals (3) traffic incidents (4) work zones (5) bad weather and (6) special events like football matches or concerts. Instead of saying congestion is caused by the travel demand exceeding the road capacity, you could just as well say that congestion is caused by the capacity dropping below the travel demand for any of these reasons. While some of the disturbances like bottlenecks and poorly functioning traffic signals are related to a specific location, disturbances like bad weather, incidents and special events are unpredictable. They can occur at any time and at any location.

Even beyond these physical and random influences, congestion can be considered a disturbance in itself. A so called 'wide moving jam' is typically a short jam that propagates in the opposite direction of the traffic. The short jam usually originates at a 'weak link' of any specific road. An example of such a weak link is the location where four lanes become three lanes and people are asked to merge. The jam can move through bottlenecks and different traffic stages with a speed that is constant on average.

---

[1] INRIX analyzed the data of some 100 million drivers using GPS. INRIX® is a leading provider of traffic information and intelligent driver services.

If the flow of traffic driving into the wide moving jam is equal to the flow driving out of the jam, it will stay intact. A wide moving jam can travel distances up to 15km, considering the wide moving jam usually moves through traffic with a speed of 15/20 km/hr, it can be active for an hour or even more. The general rule is that the outflow of traffic in a wide moving jam is 30% lower than the free capacity of the road. This means that the realized capacity of the road can be much lower than the theoretical capacity. A very well-known example of this in the Netherlands is the freeway route A13-A20-A16 which passes Rotterdam.
This route is known to be one of the most congested routes in The Netherlands. It has been shown that a large part of the congestion on the A13 is caused by moving jams [Vonk Noordegraaf, 2013].

Wide moving jams are often explained by Kerners three-phase traffic theory [Kerner, 1993]. In short a wide moving jam is a special type of congestion that is caused by the imperfect driving style of road users under instable traffic conditions. This type of congestion can be classified as an operational bottleneck; there is no physical reason for the low capacity at this location, it is a consequence of inefficient use of the system by its participants. Hegyi cites a Japanese study [Sugiyama, 2008] where an experiment was carried out with vehicles driving on a circular road with equal speed and following distances. They discovered that after a while, almost invisible disturbances, like a small fluctuation in speed, would develop into a wide moving jam. According to this theory such a jam can pop up everywhere, that is why these jams are sometimes referred to a phantom jams. As is stated by Hegyi and van de Weg: ‘’Phantom jams don’t exist’’ [Hegyi, 2014]. What is meant with this statement is that the type of jam, the wide moving jam, which the phantom jam refers to does exist but they are not in fact ‘’phantom’’. This is easily proven by the simple fact that the starting point is constant. The Japanese experiment was carried out in a situation where speed and density are higher than we experience in real life. Often there is a combination of factors that contribute to the formation of a wide moving jam. Speed and density are high but there is another specific reason (or more) at play.

The SPECIALIST[2] algorithm developed at the TU Delft has been successful in practice on the A13 to solve wide moving jams [Hegyi, 2008]. The SPECIALIST algorithm can actively detect a wide moving jam and solve it by creating an imbalance between jam in- and outflow. The control input comes from detection loops or road side speed portals.
The latest development based on the same insights, the COSCAL algorithm, has the ability to combine road side data with in-car data.

[2] SPEed Controlling ALgorIthm using Shockwave Theory.

Although these algorithms have proven themselves to be successful there lie a lot of challenges ahead. It has been studied that variable speed signs change the lane distribution, which directly effects the capacity and possibly cause congestion elsewhere [Knoop, 2010]. Knoop studied the effect of speed on lane utilization and concluded the impact to be in the same order of magnitude as the initial problem. A lower speed limit will cause more vehicles to utilize the outside lane, which is better for the capacity, but there is a downside as higher density on the outside lane disturbs the merging process. As a consequence ramps can become congested or shockwaves can develop into a wide moving jam. That is why Hegyi and van de Weg promote a broader perspective, wide moving jams should be tackled considering the entire trip to evaluate the collective efficiency.

Instead of cutting off the flow to solve the moving jam why not stimulate the flow at the known locations where they originate? In this thesis it is proposed to solve the operational bottleneck that causes a wide moving jam by stimulating vehicles to maintain their speed. At the origin of a wide moving jam a dynamic road sign will be placed that displays your speed with a ☹ if you are driving too slow and a ☺ if your speed is ok.

To study the effect of this measure a fundamental diagram is made of the A-13 by fitting empirical data. A simple simulation model is proposed and calibrated with the fundamental relations in traffic flow theory. Since the results are highly dependent on the compliancy of the road users to increase their speed, multiple scenarios are considered. Finally microscopic and macroscopic results are evaluated and recommendations are discussed.

1.1 Problem statement

It has been shown that wide moving jams are responsible for a large part of the traffic delay we experience. The general approach in tackling wide moving jams is to reduce the oncoming traffic flow at the locations where wide moving jams often originate. The problem here is that the control measure can set into motion a chain of events that causes congestion somewhere else in the network.

1.2 Research question

This thesis aims to study the effect of stimulating road users to maintain their speed at an operational bottleneck. The stimulation will be done by installing a road sign that displays the slower vehicles with a sad smiley face, ☹ and a happy one, ☺ if the speed is sufficiently high.
The idea behind the smiley signs is to encourage vehicles to pay extra attention to their speed.

Compared to control measures that restrict flow, the proposed idea is far less invasive on traffic. Instead of relieving a wide moving jam by restricting the inflow, it is proposed to cancel out the operational bottleneck by encouraging vehicles to increase their speed. This leads to the following research question:

‘‘Can a smiley traffic sign encouraging drivers to increase their speed be implemented to prevent wide moving jams?’’

To answer this question some sub questions are formulated. As the proposed solution is intended to have drivers increase their speed to avoid the formation of slow moving jams, the first sub question is; does the lowering of speed at some specific location indeed lead to slow moving jams? Furthermore, the effectiveness of the smiley sign is highly dependent on the compliancy of the road users. Therefore an important question is; to what degree does the effectiveness of this stimulation measure depend on the compliancy of the road user?

1.3 Overview

This thesis will start with an introduction on Traffic Flow Theory. Microscopic and macroscopic characteristics and models are introduced. As well as some phenomena that are observed in Traffic Flow Theory and which are important concepts in analysing congestion.

To study the effect of a speed stimulating control measure the highly congested A13 is studied as a case example. This Dutch highway is known to have certain bottleneck locations where drivers tend to lower their speed for no apparent reason. In Chapter 0, one of these locations where wide moving jams typically form is analysed. Chapter 4 introduces the microscopic simulation model that is proposed to study the effect of the proposed stimulation measure. In Chapter 5 the simulation setup and results will be discussed. This thesis will end with a conclusion and recommendations for future research.

2 Traffic flow theory

The first traffic flow models were developed from an intuitive mathematical modelling point of view. It was only until later when phenomena like congestion and queuing started to play a more prominent role, then it was recognized these phenomena studied in traffic flow theory needed to be incorporated to be able to more realistically model traffic flow operations. By definition emerging phenomena are higher level structures that arise through the interaction of lower level entities that themselves do not exhibit such properties. In traffic flow modelling, this characteristic of phenomena makes it hard to predict and describe traffic flow operations. With the equations of motion each individual vehicle can be described as a function of time but a traffic jam cannot.
This chapter starts with an introduction to the study of Traffic Flow Theory. In Paragraph 2.2 the wide moving jam is explained by means of Kerners three phase flow theory and in Paragraph 2.3 the concept of capacity and the capacity drop phenomenon are discussed. This is followed by an overview of both microscopic and macroscopic traffic flow models. These are important for further reading and analysing the results.

2.1 Traffic Flow Theory

In [Hoogendoorn, 2004] the study of Traffic Flow Theory is described as follows:

‘’Traffic flow theory pertains to The Knowledge of Fundamental Traffic Flow Characteristics and Associated Analytical Techniques.’’’

Fundamental Traffic Flow Characteristics are properties of individual vehicles like vehicle trajectories, headways and speed or properties of a traffic stream like flow density and mean speed. Here we begin by making a distinction between microscopic and macroscopic characteristics. Properties of individual vehicles are microscopic characteristics and properties of a traffic stream are macroscopic characteristics. Figure 2.1 shows an example of vehicle trajectories in a time space diagram. Vehicle trajectories provide a very clear insight into traffic flow conditions, all information a traffic analyst requires can be determined from the trajectories: individual speeds and acceleration (microscopic characteristics) but also macroscopic flow characteristics. In Figure 2.1 the microscopic characteristics are illustrated. Time headway, denoted by h_i, is defined as the period of time between the passing moment of the vehicle considered and the preceding vehicle. The distance headway, s_i is the distance at one time instance between the rear bumper of the vehicle considered and the preceding vehicle. The speed $v_i = dx_i/dt$, is the tangent of the trajectory and acceleration is defined by $a_i = d^2x_i/dt^2$.

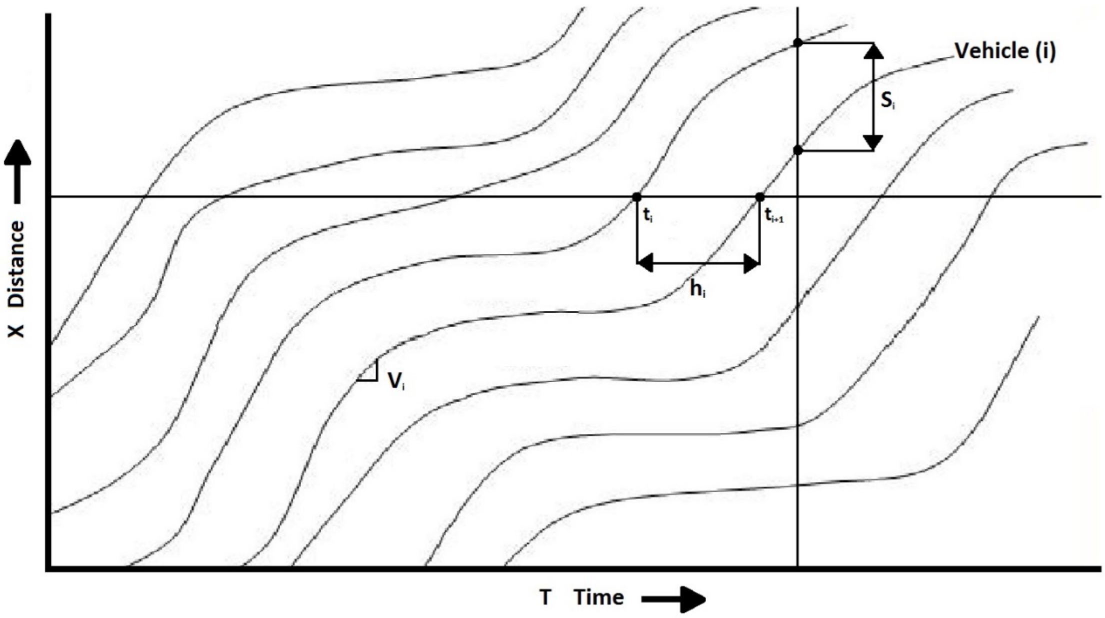

Figure 2-1 Vehicle trajectories in time space diagram.

Macroscopic characteristics make no distinction between individual vehicles but describe the traffic stream as a whole. The three main macroscopic variables, flow, density and mean speed describe average behaviour of the traffic stream. Because of the aggregate nature of the macroscopic characteristics, they can all be derived from the time space diagram in Figure 2.1. Flow is the number of vehicles per time unit, density is the number of vehicles per space unit. The mean speed can be determined by averaging all individual speeds at one cross section, this is the so called local mean speed or spot speed. This is the mean speed that will be considered later on in Chapter 4 when empirical data from the A-13 is analysed.

There exist many different techniques to analyse traffic flows. The techniques that are covered in this thesis are; Microscopic simulation models, Macroscopic traffic flow models, Queuing analysis and

Capacity analysis. Furthermore, we can distinguish between deterministic and stochastic models. The models will be discussed after the following paragraphs which entail the traffic flow phenomena queueing, or more specifically the wide moving jam, and the concept of capacity including the capacity drop phenomenon.

2.2 Queueing: The wide moving jam.

The concept of the wide moving jam can be explained with the use of Kerners three phase traffic theory. Kerner [Kerner, 2003] suggests there are three phases in traffic: free flow, synchronised flow and wide moving jam. Previous theories defined just two phases namely the free flow phase and the congested phase. Kerner specifies two congested phases, the first one is the synchronized flow phase, there is congestion but there is still a continuous flow although speed is decreased. In this phase the speed on the freeway lanes is more or less equal as there are no overtaking opportunities. Another characteristic of synchronized flow is the usually fixed downstream front of the congestion, see Figure 2-2. Synchronized flow typically occurs at bottleneck locations where the downstream front of the synchronized flow is fixed at the bottleneck location. The downstream front where vehicles accelerate out of the synchronized flow phase into the free flow phase is constant, see Figure 2-2.

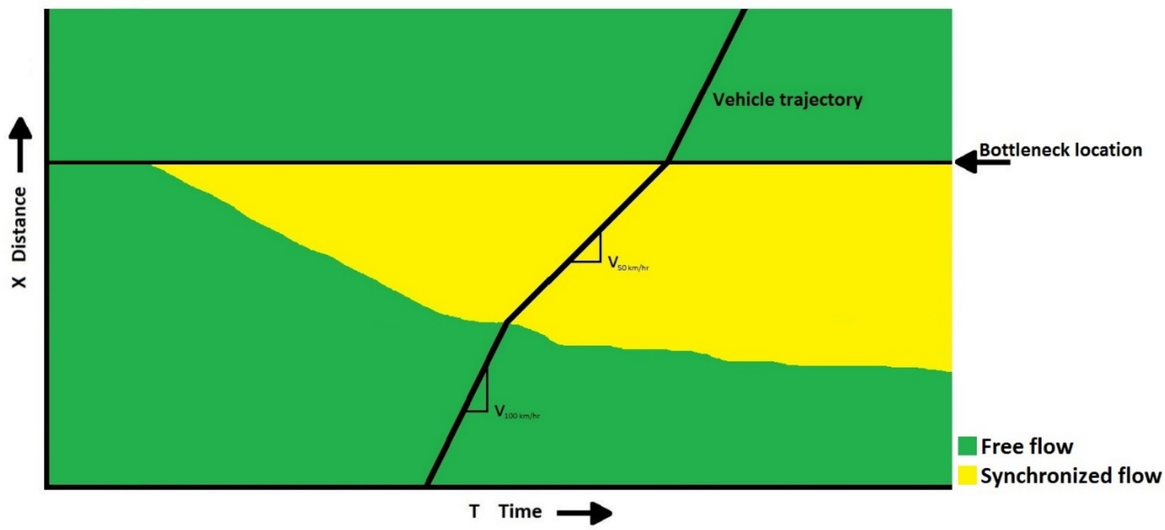

Figure 2-2 Synchronized flow in time space diagram with fixed downstream front at bottleneck location.

Another notion Kerner makes is the existence of multiple steady states. Steady states are hypothetical spatially homogenous and time independent traffic states. As a consequence the flow density relation in Kerners fundamental diagram is not a line but an area as seen in Figure 2-3. The line marked F in

Figure 2-3, describes the free flow phase, the maximum free flow density and flow rate are marked, respectively, $\rho_{max}^{(free)}$ and $q_{max}^{(free)}$. The synchronized flow phase is the shaded area $q_{max}^{(free)}$ which is the maximum flow that can be achieved in this phase. $V_{min}^{(syn)}$ is the minimum speed in the synchronized flow phase, it is equal to the slope of the dotted line that runs from the origin of the diagram to the lower boundary of the synchronized flow area in Figure 2-3.

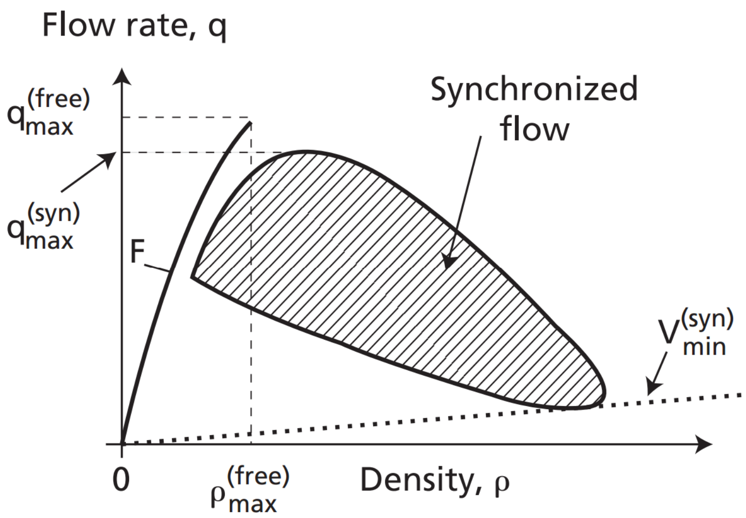

Figure 2-3 Fundamental diagram of Kerners three phase traffic flow [Hoogendoorn 2012].

The wide moving jam is the second congested phase. This phase can be recognized by the stopped or nearly stopped vehicles inside the jam and the ‘‘moving’’ property. Considering the downstream jam front, where vehicles can accelerate, it propagates through traffic with the mean velocity of the front. Figure 2-4 shows how the wide moving jam, represented by the ‘‘stopped cars’’, moves in the opposite direction of the vehicles. In time, from $t = 0\ s$ to $t = 18\ s$, the vehicles move from left to right and the wide moving jam moves from right to left.

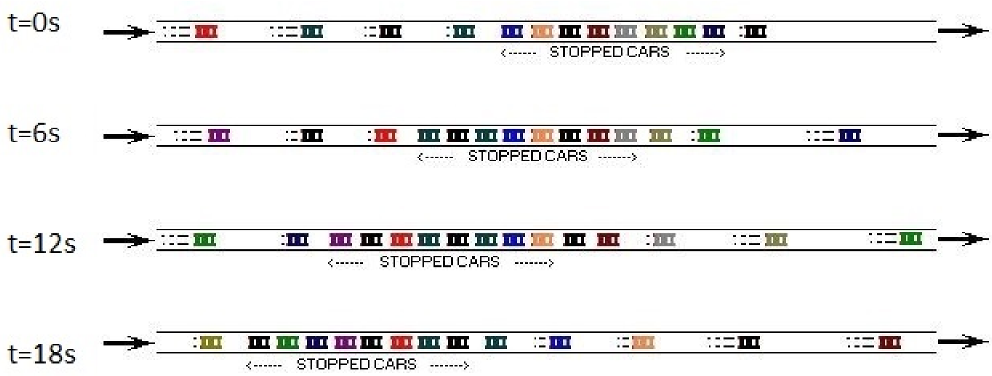

Figure 2-4 Representation of a wide moving jam propagating through traffic.

The wide moving jam has the ability to travel through bottlenecks and complex traffic states while keeping the mean velocity of the front.

As long as the flow at the upstream jam front, the decelerating vehicles approaching the jam, is equal to the flow at the downstream jam front the wide moving jam keeps propagating through traffic with the mean speed of the accelerating vehicles at the downstream jam front. This is a characteristic parameter of a wide moving jam as is does not depend on flow rates and densities upstream or down stream the jam front. It can be seen that at the downstream jam front vehicles accelerate one by one with a time delay that ensures a safe driving distance to the preceding vehicle. Figure 2-5 shows how the mean speed of the wide moving jam can be calculated under some conditions. Suppose that the percentage of long vehicles, weather and driver style are constant, then the mean density $\bar{\rho}$ and the mean delay time between vehicles accelerating $\bar{\tau}$ are constant. With these assumptions the mean wide moving jam speed $\bar{v}_{jam}$ is 5 m/s or 18 km/hr in the example of Figure 2-5.

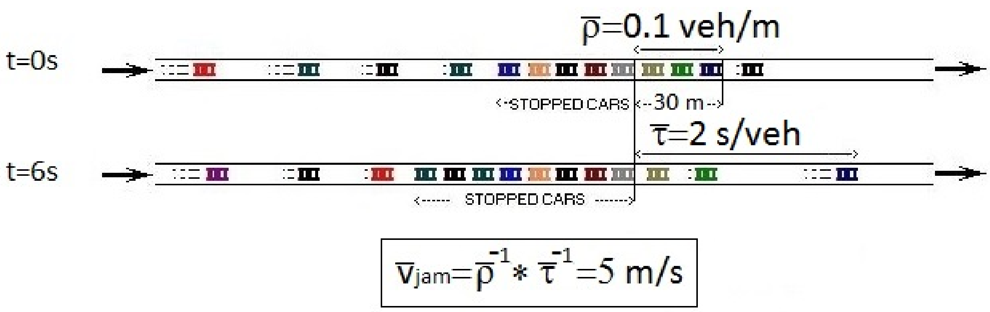

Figure 2-5 Example of mean speed of a wide moving jam.

The existence of wide moving jams holds a close relation to the stability of traffic. Kerner states that, within a certain density range, the steady states in the fundamental diagram are unstable. The stability of traffic is classified by the way perturbations affect the flow. Stable traffic flow states can resist a wide range of perturbations. In the free flow phase one vehicle breaking too hard will not likely cause a phase transition. In the free flowing phase vehicles are by definition driving their free or desired speed and are not restricted by preceding vehicles. In this phase overtaking opportunities are present which acts as a buffer for perturbations. When the percentage of vehicles that are restricted increases, the overtaking possibilities are decreased and the more likely it is that a perturbation will cause congestion. In this traffic state where vehicles are following, the headways are minimal and one vehicle breaking too hard can cause a wide moving jam as the perturbation grows in amplitude. This means that vehicles upstream of the vehicle breaking too hard brake even harder. Vehicles driving with a minimum headway instinctively want to keep this distance between themselves and the preceding vehicle. In case of the preceding vehicle braking, the distance to that vehicle is already decreased because of the reaction time and therefore there is a tendency to brake harder.

2.3 Capacity

Road capacity is an important concept since it is the main parameter used in performance functions to calculate travel times and delay times.
The most widely used term for capacity is adopted from The Highway Capacity Manual [TRB, 2000] which defines capacity as follows:

''the maximum sustainable flow rate at which vehicles or persons reasonably can be expected to traverse a point or uniform segment of a lane or roadway during a specified time period under given roadway, geometric, traffic, environmental and control conditions; usually expressed as vehicles per hour, passenger cars per hour, or persons per hour'' [TRB, 2000].

Note here that in practice several issues arise which make it complicated to define capacity as is proposed. An example of this is the capacity drop phenomenon as described in the next section.
The capacity drop is characterised by a discontinuity in capacity before and after a queue. Typically the capacity before a queue is higher than the capacity after a queue, called the queue discharge rate. The magnitude of capacity drop varies over a wide range depending on the local traffic conditions such as number of lanes and traffic composition as well as speed inside the congestion as studied in [Yuan, 2014].

2.3.1 Capacity drop

Edie was the first researcher to suggest a discontinuity between the capacity before a queue and the capacity after a queue [Edie, 1965]. He observed that when vehicles are moving out of a state of congestion into capacity this capacity is lower than when vehicles are moving from a state of free flow into capacity. In Figure 2-6 this idea is illustrated, where the free flow branch reaches a higher capacity than the congested branch. Respectively these two maximum flow rates are called the pre-queue capacity and the queue discharge rate. In Figure 2-6 the pre-queue capacity is q_{c1} in and the queue discharge rate is q_{c2} in veh/hr for the same density k_c in veh/km, hence the discontinuity.

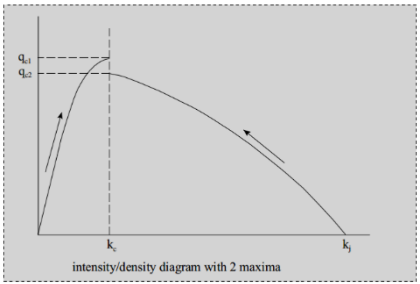

Figure 2-6 Fundamental diagram with discontinuity, with density k in veh/km and flow q in veh/hr.

To determine the pre-queue maximum flow rate, by definition, the maximum flow rates are observed at the downstream location of congestion just ***before*** the congestion sets on.
The maximum flow rates observed in this situation are characteristically showing a large variance, the speed is high and traffic is unstable hence the on-set of congestion upstream [Minderhoud, 1999].
The queue discharge rate is the maximum flow rate observed at the downstream location of congestion from when congestion has set on until as long as the congestion exists. Opposed to the maximum flow rate observed pre queue, the maximum flow rate of vehicles transitioning from a state of congestion into a state of free flow is characteristically lower and the variance is smaller.
Both capacities can only be measured downstream the bottleneck location because by definition a bottleneck determines, in this case, the capacity of a linked system.
In Figure 2-2 for example both maximum flow rates are measured at the same location just above the bottleneck. In time, the pre queue capacity is the maximum flow measured before congestion and the discharge rate is the maximum flow measured as long as the congestion is present.
The differences between the two capacities, the capacity drop, are in the range of 1% to 15% [Hoogendoorn, 2004]. Different explanations for the capacity drop are discussed in literature. Dijker argues that the main reason is the preference for larger headways if drivers experience congested

conditions [Dijker, 1998]. Differences between acceleration and deceleration behaviour are also expected to contribute to this phenomenon.

2.4 Microscopic and Macroscopic models

In this thesis a specific location on the A-13 is taken to analyse the origin of the wide moving jam. To this end empirical data is used that contains information about mean speed, flow and density. These are typical macroscopic parameters. To analyse the effect of the smiley sign a microscopic simulations model is proposed in Chapter 5. Therefore it is important to explain both the concept of microscopic and macroscopic characteristics and models.

In the study of traffic systems a key distinction is made between microscopic and macroscopic characteristics. Microscopic characteristics pertain to the individual driver-vehicle unit. Examples of microscopic characteristics are time headways, individual speeds, and distance headways. Similarly, microscopic models describe the behaviour of individual drivers, for instance in relation to the infrastructure and other drivers in the traffic flow. That is, they predict the behaviour in terms of microscopic characteristics. Typical analytical techniques are headway distribution modelling and microscopic simulation models. On the other hand, macroscopic characteristics pertain to the properties of the traffic flow as a whole (for instance at a cross-section, or at a time instant). Examples of macroscopic characteristics are: flow, time mean speed, density, and space-mean speed. One must keep in mind that although the representation of traffic may be macroscopic, the rules predicting the dynamics of the traffic flow may be based on individual driver behaviour and while microscopic models represent all vehicles in the traffic flow individually, this does not necessarily mean that the behaviour of the vehicles is based on microscopic rules.

2.4.1 Microscopic models

Microscopic traffic flow models describe the behaviour of the individual driver. Both the interaction of the driver with the road or environment and the interaction with fellow drivers. The advantage of this type of modelling is that the complete information about the state of each vehicle is known, it is easy to assign various characteristics to the vehicle or driver. For example driving style, a driver can be patient or aggressive which will affect the behaviour under different circumstances.
However this high level of detail, where the behaviour of every individual entity in the system is described makes microscopic models computationally very intensive. The two most important aspects

of the microscopic traffic models are the so called car following and lane changing behaviour, generally described as functions of headway, relative speed or the ratio between following speed and desired speed. As in this thesis a one lane model is utilized for simulations in Paragraph 2.4.1.1 car following models are discussed. These models are applicable to relatively busy traffic where the overtaking possibilities are small and drivers are restricted by the vehicle in front of them. In Paragraph 2.4.1.2 and 2.4.1.3 two more types of microscopic models are described in the category of the Netlogo simulation model in Chapter 4.

2.4.1.1 Car-following models

Car following models are dynamic models that describe the action of a vehicle relative to the vehicle in front as a function of headway, relative speed etcetera. Many vehicle following models are discussed in literature, and many of these are based on anti-collision concepts. A well-known model of this type is the Gipps model, developed in 1981. It assumes that a vehicle always aims to be able to stop safely if its leader performs an emergency stop. The speed is updated using the current speed, desired speed, maximum acceleration, maximum deceleration and headway of the following vehicle plus the current speed of the followed subject vehicle. Every instance two possible values for the updated speed are calculated; one based on the drivers desired speed limited by vehicle performance, and one based on safety, being the speed that ensures there is no collision. The minimum of these two is selected as the speed the following vehicle proceeds with and thus satisfying both limitations.

2.4.1.2 Cellular automaton models

CA models which stands for Cellular Automata models are discrete dynamical systems. The roadway is divided into small cells that can either be occupied by one vehicle or not. As both time and space are discrete variables it follows vehicle speed, acceleration and deceleration are discrete as well. Despite this rather coarse representation, the CA-model describes the dynamics of traffic flow fairly well [Hoogendoorn, 2004]. The updating of the vehicle dynamics is achieved using the following rules:

- 1. Acceleration. If a vehicle has not yet reached its maximum speed and if the distance to leading vehicle permits it.
- 2. Braking. If the distance headway is smaller than minimum safe distance. The minimum safe distance is a discrete function of speed, for example the safe distance is equal to the speed multiplied by the simulation time step.
- 3. Randomisation. To describe the imperfection of vehicle following behaviour a random variable is introduced that lowers the speed by over writing the rules.
- 4. Convection. The vehicle will move ahead with a certain number of cells during a single time step.

Due to the simplicity of the model, complex networks with a large number of vehicles can be simulated in real-time. The CA model is able to describe the spontaneous formation of traffic congestion when speed and density are high or in other words flow conditions are unstable. A large number of modifications and additions to the basic rules given here are possible including lane changing rules etcetera.

2.4.1.3 Agent based models

Agent Based models or often abbreviated ABM represent a system in a way where agents interact with each other and their environment using a set of rules.
Agent based models differ from other component modelling systems such as cellular automata from Paragraph 2.4.1.2 by the continuity of the landscape, the heterogeneity of components, and the stochastic influences in agent motion and interaction.

2.4.2 Macroscopic models

A Macroscopic traffic flow model is a model that describes traffic in terms of macroscopic characteristics like density, flow, mean speed of a traffic stream, etcetera. It describes the fundamental relation of traffic flow. These relations are useful to determine optimal network conditions, by operating the system at its peak capacity, where it functions most efficiently. Another use of this type of model is to determine trip times by the flow density relation. As opposed to modelling each vehicle individually, as is done in microscopic studies, individual vehicles are represented in an aggregate manner. Since the exact fundamental relation between speed, density and flow are unknown, there exists a wide variety of models. Macroscopic models can, for example, be obtained by aggregating microscopic models or by fitting empirical data. Although outdated, models based on the analogy with fluid or gas streams have been constructed. Because the behaviour of the road participants cannot be predicted in the same way that the behaviour of fluids or gas can be predicted, these models have limited use in real-life situations. In this paragraph one of the simplest macroscopic traffic flow models is given, proposed by Greenshields. Also more realistic models and the modelling of stochastics involved in traffic flow are discussed.

Developing macroscopic models is one of the primary approaches to modelling complex systems. Macroscopic models follow a top-down approach, these simulations have the advantage that run-time can be fairly short and are helpful when only a coarse prediction of conditions is sufficient.

2.4.2.1 Greenshields model

Greenshields [Greenshields, 1934] proposed the use of a linear function to summarize the speed-density relation. Such a function can be completely determined by knowing two points on the line:

- Density, $k = 0$ and speed v, is equal to free flow speed, v_f
- Speed, $v = 0$ and density k, is equal to the jam density, k_j

The speed-density relation in Figure 2-7 can be expressed as:

$$v = v_f(1 - \frac{k}{k_j})$$

Equation 2-1

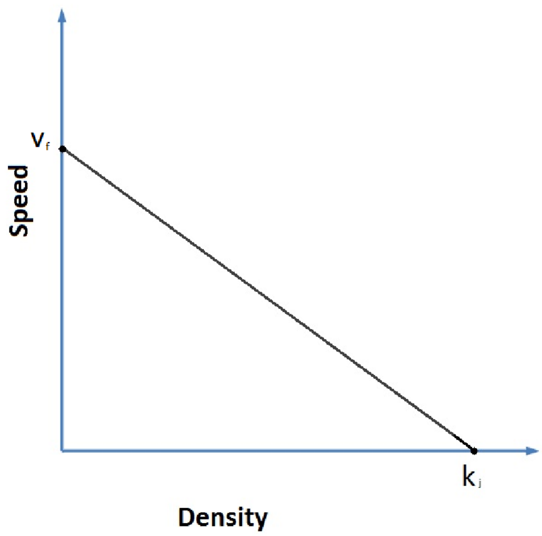

Figure 2-7 Linear speed density relation.

This is the Greenshields model [Greenshields, 1934] which depicts a linear speed-density relation. Combining the identity, $q = k * v$, one can derive the flow-density relation implied by the Greenshields model:

$$q = v_f(k - \frac{k^2}{k_j})$$

Equation 2-2

Since this is a quadratic function with a negative second order term, the corresponding flow-density curve is parabolic with a downward opening, see the bottom left subplot of Figure 2-8. Flow increases as density increases. Until, at some point, $k = k_m$, the flow peaks, $q = q_m = \frac{v_j k_j}{4}$. After this point, flow begins to drop as density continues to increase. Flow becomes equal to zero when density reaches jam density, k_j. In this notation, q_m, is the maximum flow or capacity flow and k_m is the corresponding density or the optimal density. The flow-density relation can be obtained by eliminating k from the Greenshields model with the use of the identity. Which results in the following flow-density relation:

$$q = k_j(v - \frac{v}{v_f})$$

Equation 2-3

In Figure 2-8 the fundamental diagram as proposed by Greenshields is displayed. Three conditions in traffic flow can be distinguishes:

- Stable condition, when vehicles can move with free-flow speed, v_f.
- Congested condition, in the worst case, $v = 0$.
- Optimal flow condition, q_m gives the optimal speed, v_m.

Figure 2-8 depicts all relations discussed above, namely, from left to right, the speed-density relation, flow-density and the speed-flow relation. A model (and its associated graphical representation) that summarizes the pair-wise relations among traffic flow characteristics is referred to as the fundamental diagram in traffic flow theory. The Greenshields model (including the graphical representation as depicted in Figure 2-8) constitutes the first fundamental diagram in traffic flow theory.

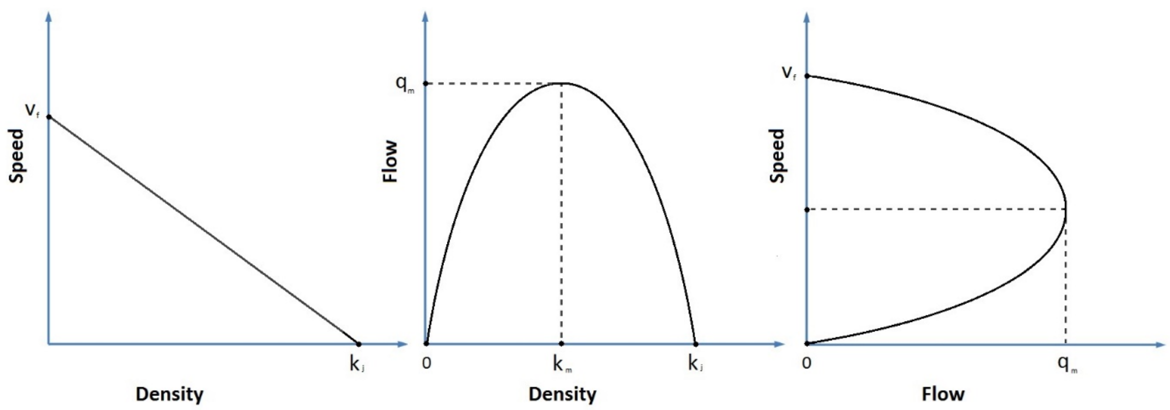

Figure 2-8 Greenshields fundamental diagram.

2.4.3 Stochastic modelling

Though all relations presented before take deterministic forms, the actual relations are essentially statistical. Figure 2-9 and Figure 2-10 illustrate the scattering effect of empirical observations and how deterministic models fail to capture such an effect [Ni, 2015]. Therefore, a step forward to advance the modelling of the fundamental traffic flow relations is to consider the scattering effect by representing speed as a distribution at each density level, instead of a fixed number. This idea is visualized in Figure 2-10, the different coloured probability density functions show the estimated mean and deviation of the empirical observations and how they vary over the deterministic speed/ density relation.

Ni proposes to define speed as a distribution function at each density level and thus turning the speed/ density relation into a stochastic relation. Empirical observations seem to support such a proposition [Ni, 2015]. A study of such a stochastic model, opposed to the deterministic one, has shown that although deterministic speed/ density relation models can explain physical phenomena underlying fundamental diagrams, the stochastic model is more accurate and more suitable to describe traffic phenomena [Wang, 2009].

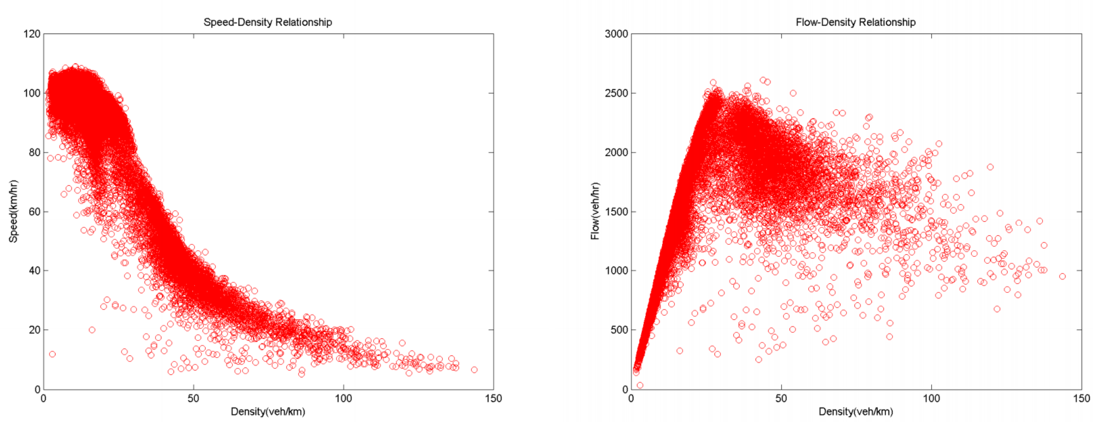

Figure 2-9 Scattering effect of the fundamental relation [Ni, 2015].

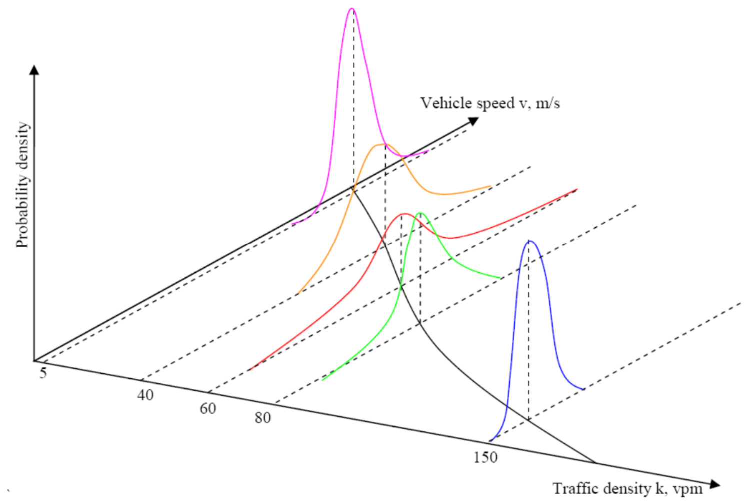

Figure 2-10 Illustration of stochastic speed/ density relation [Ni, 2015].

2.5 Summary

In this chapter important concepts from Traffic Flow Theory were discussed. These concepts will be used throughout the rest of this thesis and applied to the well-known route on the A13 were slow-moving jams tend to form. In the next chapter this route will be discussed in more detail.

3 Fitting a macroscopic model to the A13

3.1 Introduction

The Dutch motorway A13 is a 17km long motorway that connects Rotterdam and Den Haag. It is often high ranked in listings about the most congested routes in the Netherlands. Vonk Noordgraaf has established that a large part of the congestion on this motorway is caused by wide moving jams [Vonk Noordgraaf, 2013]. These are sometimes referred to as phantom jams because they seem to pop up for no apparent observable reason. Practically all studies on the subject agree on one thing, namely: wide moving jams form when speed and density are high or in other words, when traffic operates at critical stability. Theoretically a wide moving jam could form by just these two ingredients but often there are other factors that contribute to this type of congestion. Observations show there must indeed be a contributing factor that has to do with infrastructure or environment since wide moving jams have a specific starting location.

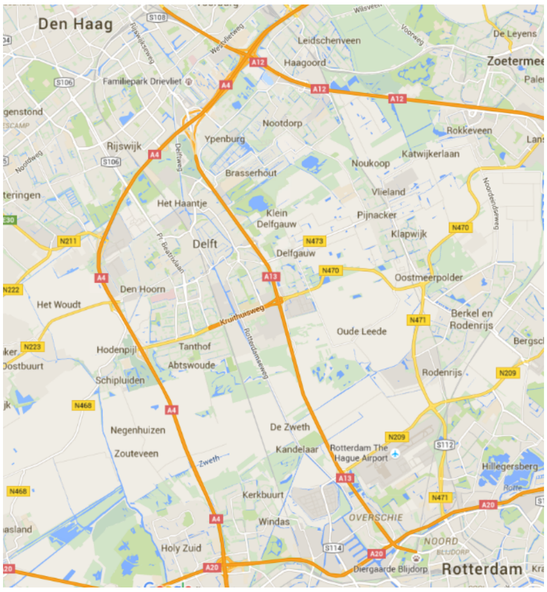

Figure 3-1 A13 from Google Maps

A-13 has a ''peak'' intensity or flow of 60.000 vehicles per hour. Figure 3-2 shows the Dutch road network with the A-13 highlighted in red. Each road is made up of links between so-called detector loops. The detector loops count the vehicles and measures the speed. The dataset used here is 15 minute data, which means measurements are aggregated into intervals of 15 minutes each containing the vehicle count and the mean speed within that specific interval.

Figure 3-2 Dutch motorway network with the A13 in bold, main roads.

In this chapter the situation on the A-13 will first be discussed in more detail. From the data of specific links on the A-13 some empirical observations are deduced and validated in paragraph 3.2. The chapter will conclude by fitting the data to a macroscopic model.

3.1.1 Wide moving jam on the A13

Figure 3-3 [Yuan, 2010] and Figure 3-4 [Hegyi, 2014] show wide moving jams that originate from the same location on the A13. Only the orientation of the figures is different. In Figure 3-3 the wide moving jam travels up the page from left to right in time, towards Delft North at 6.5 km. The y-axis is the road location in km, the vehicles travel from Delft North $(6.5\ km)$ to Rotterdam Airport $(14.5\ km)$. The x-axis represents the time in hours and the colours stand for the mean speed on the road, green is $100\ km/hr$ and red is $0\ km/hr$. The wide moving jams can be recognised by the red lines. It can be seen how they move up in time from left to right. In this particular case a lot of wide moving jams form over time and travel about 7 km where they transition into a long traffic jam.

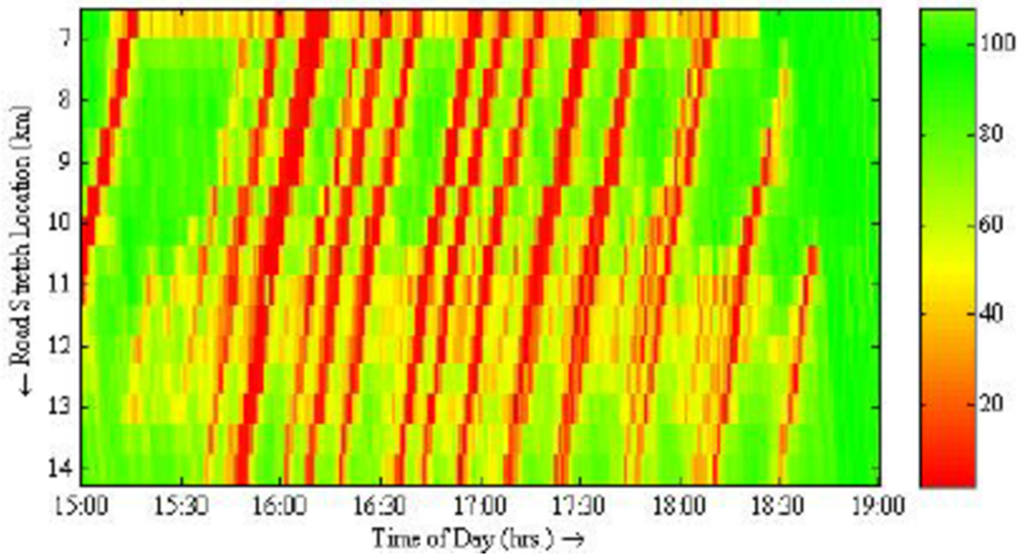

Figure 3-3 Contour plot of the A13 between Delft North (6.5 km) and Rotterdam Airport (14.5 km), southbound [Yuan, 2010].

In Figure 3-4, the jam also travels towards Delft North in time from left to right but in this figure Delft North lies down the page. In this figure one wide moving jam can be seen, in this case black is a mean speed of $0\ km/hr$ and yellow marks a mean speed of $100\ km/hr$. The y-axis is again the road location in km but this time the driving direction is up, as depicted by the black arrow. From left to right in time the wide moving jam starts between $15\ km$ and $16\ km$ and moves down the page. Around $6/7\ km$

the wide moving jam dissolves, this means the inflow of the jam is less than the outflow of the jam. It can be seen in the figure how the wide moving jam is thinner near the end, this means the time vehicles are actually stopped inside the jam is shorter. Around $12{:}15\ hr$ the wide moving jam stops propagating through traffic, it then remains stationary in time. As from this moment first the mean speed in the jam increases, see the colour changing from blue to purple to red which indicates a mean speed change from $20\ km/hr$ to $40\ km/hr$ to $60\ km/hr$.

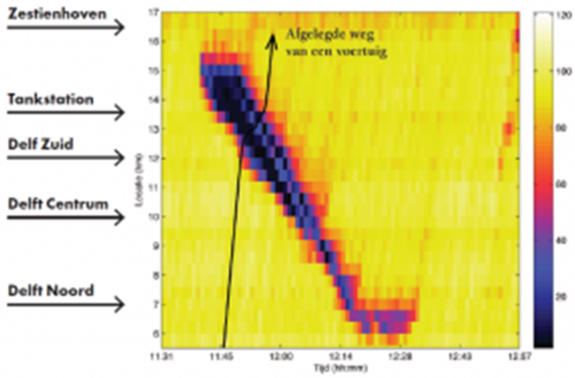

Figure 3-4 The same scenario as Figure 3 3, wide moving jam traveling from Zestienhoven to Delft Noord (different orientation) [Hegyi, 2014].

Both these pictures show the same situation only at a different time, where a wide moving jam develops at approximately the same location.

To take a closer look at this part of the road where wide moving jams seem to develop, see the next satellite pictures from Google Maps (Figure 3-5, Figure 3-6 and Figure 3-7). Figure 3-5shows an image from Google Maps between respectively, from top, to bottom, the Petrol Station between $13\ km$ and $14\ km$ and the Rotterdam Airport location at just about $16.5\ km$.

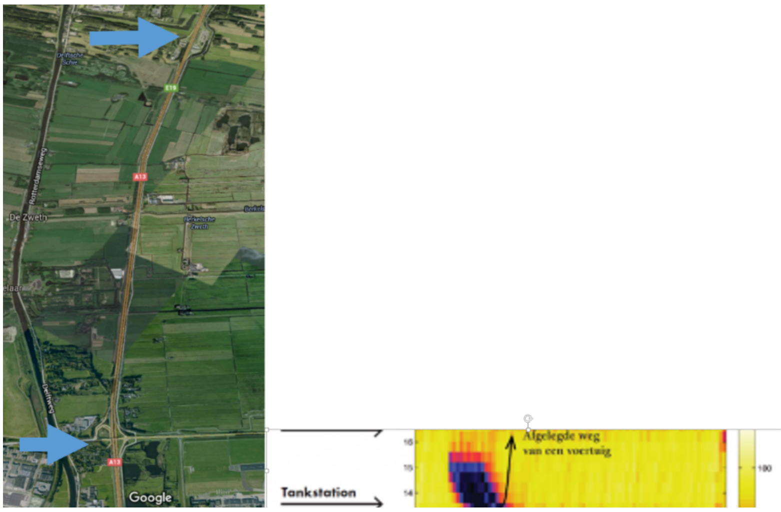

Figure 3-5 Left figure: Top to bottom, Petrol Station at $13.2\ km$ *and Rotterdam Airport at* $16.4\ km$

Right figure: reference picture of where the left figure is situated in Figure 3-4.

Figure 3-5 shows the road segment between the Petrol Station and Rotterdam Airport where the wide moving jam starts between $14\ km$ and $15\ km$. This road segment between the Petrol Station and Rotterdam Airport counts two detector loops. Figure 3-6 and Figure 3-7show these two links with their satellite image on the left.

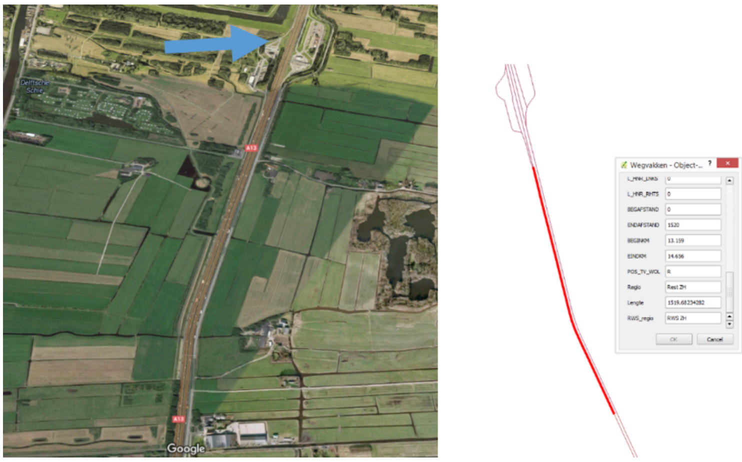

Figure 3-6 Link 137288026 top to bottom, $13.2\ km$ *at the petrol station and* $14.7\ km$ *with satellite image.*

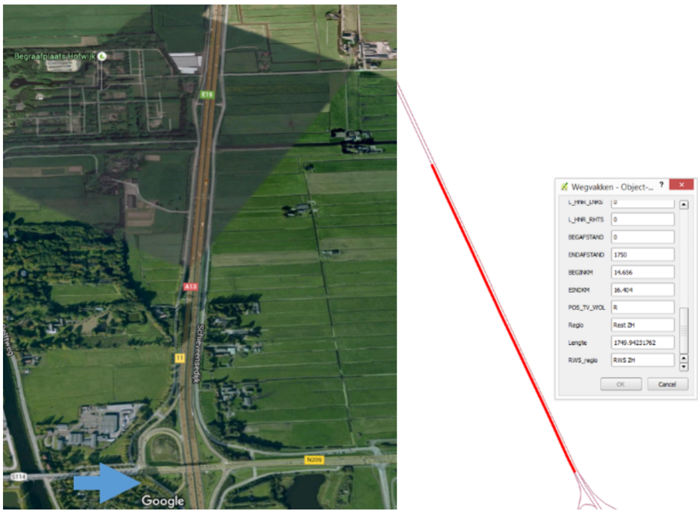

Figure 3-7 Link 174284007 top to bottom, $14.6\ km$ and at $16.4\ km$ Rotterdam Airport with satellite image.

From contour plots as Figure 3-3 and Figure 3-4 it can be seen where the origin of the wide jam is, study has shown how wide moving jams typically have a constant starting point [Hegyi, 2014].
The question is why at this particular location? Looking at the two links, from the satellite figures, no infrastructural or environmental differences seem apparent except for the small wooded patch near Rotterdam Airport. Bad vision will lower the capacity which could explain why wide moving jams start at this location. In the remaining part of this chapter the empirical data of two links is analysed to establish the differences in behaviour depending on these links.

3.1.2 Detector loop data

Roadside traffic information systems collects time-stamped traffic counts with vehicle classification, this is done based on the weight, so for instance a truck and a passenger car would be in different categories. Vehicle instantaneous speed and headways are registered, the latter is defined as the temporal distance between two consecutive vehicles. Although every vehicle is measured, the generated dataset is macroscopic since there is always some aggregation level. The characteristics of different vehicles are aggregated within a certain time interval, this interval can be a minute, two minutes or even 15 minutes. The optimal aggregation level depends on the purpose of the data, for example, Park [Park 2007], found an optimal aggregation size of 3 to 5 minutes for freeway travel-time estimation and 10 to 20 minutes for freeway travel-time forecasting. The results he found can be regarded as a guideline because if, for example, one would only be interested in travel-time estimation at a specific time of day, the trade-off between bias and precision and thus the optimal time interval will be different. Also it has to be considered that non-ideal behaviour of the equipment and of the vehicles (think about the effect of a lane change near the loops) leads to errors in the measurements.

The state of traffic will too affect the reliability of the measurements. In a state of congestion when low speeds are measured, large errors in the intensities can occur. In literature a possible error in speed of 5% and in vehicle length of 15% is mentioned [Hoogendoorn 2004].

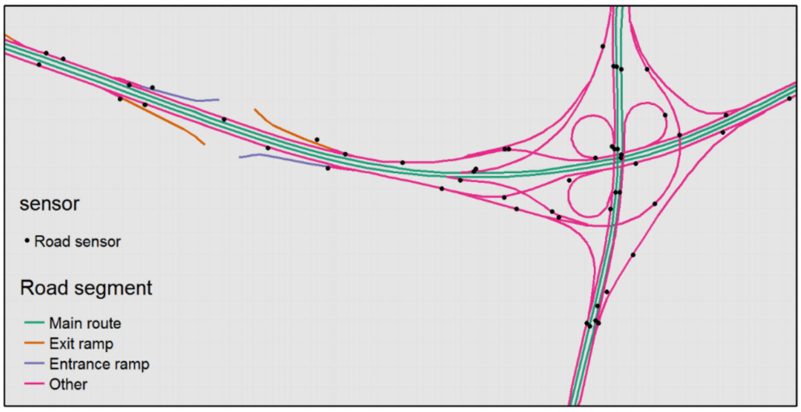

Figure 3-8 Example of a road segment with sensor loops and classification of link type [Struijs, 2014]

Figure 3-8 shows an example of how the loop network is set up. There are about 20.000 motorway detection loops in the Netherlands for different vehicle classes. Each detection loop produces one measurement per minute. To give an idea of the size of the data; this network of detection loops produces around 230 million records a day [Struijs, 2014]. In this thesis only main route data is considered as indicated in Figure 3-8. For this type of data a set of properties is given as shown in Table 3-1, for full specification of the Dutch road network see[3]. Table 3-1 shows an example of a specific link in the Dutch motorway network, a main road link, with a selection of the properties used in the NWB National Road Administration. From top to bottom, the table shows; Id, a number to identify the link, WEGBEHSRT, a letter which defines the governance under which the link falls, WEGNUMMER, a number that corresponds to the name of the motorway, WEGDEELLTR and HECTO_LTTR, both letters, in combination they give a unique location in the driving direction of the road, RIJRICHTNG, a letter that specifies the driving direction, BEGAFSTAND and ENDAFSTAND, are the start and end of the link in [m], BEGINKM and EINDKM, are the start and end of the link in [km] as part of the Hecto-interval, POS_TV_WOL, is a letter for orientation perpendicular to the driving direction.

[3]http://www.rijkswaterstaat.nl/apps/geoservices/geodata/dmc/weggeg/productinfo/beschrijvende_documentatie/Gebruikersinformatie_WEGGEG_v2.0.pdf

Specific link properties	
Id	174284007
WEGBEHSRT	R
WEGNUMMER	013
WEGDEELLTR	R
HECTO_LTTR	
RIJRICHTNG	H
BEGAFSTAND	0
ENDAFSTAND	1750
BEGINKM	14656000
EINDKM	16404000
POS_TV_WOL	R

Table 3-1 Example, detector link properties in the data set from the NWB National Road Administration.

Table 3-2 shows an example of measured information of this specific link for one time interval, of 15 minutes.

Link Traffic Table, for 06:45-07:00 hours	
Datum	04/01/2010
WVK_ID	174284007
VVU10028	1.92
VVU5028	0.00
VP28	2262.66
VMEAN28	92
Missing28	0
Unobserved28	0

Table 3-2 Example, a part of data output from the NWB National Road Administration.

From top to bottom, the table shows;

- Datum, the date, in day/month/year
- WVK_ID, a number to identify the link,
- VVU10028, VVU is the abbreviation for Vehicle Loss Hours. This indicates the collective travel time that is lost in reference to the norm indicated by the number 100 in km/hr. The number 28 indicates the counted time interval, in this particular case, interval 06:45-07:00 hours. See Equation 3-1 and Equation 3-2 for calculation.
- VVU5028, following the same principles as VVU10028, above, only the reference speed is $50\ km/hr$ and VVU50 (and VVU30) are calculated analogously.
- VP28, VP is the abbreviation for Traffic Performance, known as vehicle kilometre, defined as the intensity multiplied by the link length. In this example 2262.66 meters per hour were travelled on this specific link, between 06:45-07:00 hours so $\frac{2262.66}{4} = 565.665$ [m] were travelled at this time interval by the counted vehicles.
- VMEAN28, VMEAN is the speed mean speed in km/hr of the measured vehicles, at 15 minute time interval in number 28, thus between 06:45-07:00 hours.

- Missing28 and Unobserved28 are values that document faulty measurements or missing measurements, which is not the case in this example.

$$v_{VVU100}(a,p) = \min(v(a,p), 100)$$

Equation 3-1

$$VVU100(p) = \sum_{a} L(a)\,.\,q(a,p).\left(\frac{1}{v_{VVU100(a,p)}} - \frac{1}{100}\right)$$

Equation 3-2

With:

$v(a,p)$	Speed for measuring loop a at time interval p in km/hr.
$q(a,p)$	Intensity or flow for measuring loop a at time interval p in vehicles per hour.
$L(a)$	Length of the area corresponding to $v(a,p)$ and $q(a,p)$.

3.2 Time dependent empirical observations at the wide moving jam location and the upstream link

In this paragraph time dependent empirical observations at the wide moving jam location and the upstream link are analysed and compared. These observations will be validated in Paragraph 3.2.2 with a 4 month data set. In Paragraph 3.3 a macroscopic model is fitted following the automatic fitting procedure proposed by Knoop and Daamen [Knoop 2014].

3.2.1 24 hours observation

As discussed, the wide moving jam is often not linked to some sort of external influence or bottleneck, it seems to appear out of nowhere. However, in practice there are certain static locations where wide moving jams originate. There is no direct reason why a wide moving jam would start at this particular location, so there must be some combination of circumstances that causes the beginning of the jam in these particular locations. When speed and density are high, small fluctuations in speed can cause the onset of a wide moving jam. Since we assume here that (part) of the cause of the wide moving jam is bounded by the location, speed and speed distribution will be compared at different time instances. The link where the wide moving jam starts is shown in Figure 3-7, and the link just upstream is shown in Figure 3-6. In the rest of this thesis link 174284007 in Figure 3-7 is called the jam link and link 137288026 in Figure 3-6 is called the upstream link. During peak hours the mean speed may not be an accurate approximation of the instantaneous speed (or local mean speed see Paragraph 2.1), especially during congested conditions.

Therefore the focus here is on comparing the two links at the same time interval outside busy hours. In this paragraph one day is analysed as an example, in Paragraph 3.2.2 the conclusions are validated with a larger data set. The figure below shows an example of the mean speed measurements per 15 minutes over 1 day for both the jam link and the upstream link which is representative for the day to day situation, see Paragraph 3.2.2 for validation.

In general two peak hours can be seen, as shown by the two speed dips in Figure 3-9, one around 06:00-09:00 o'clock in the morning and another one around 14:00-20:00 in the afternoon/ evening. The figure shows that outside busy hours the mean speed on the upstream link is typically higher than the speed on the jam link.

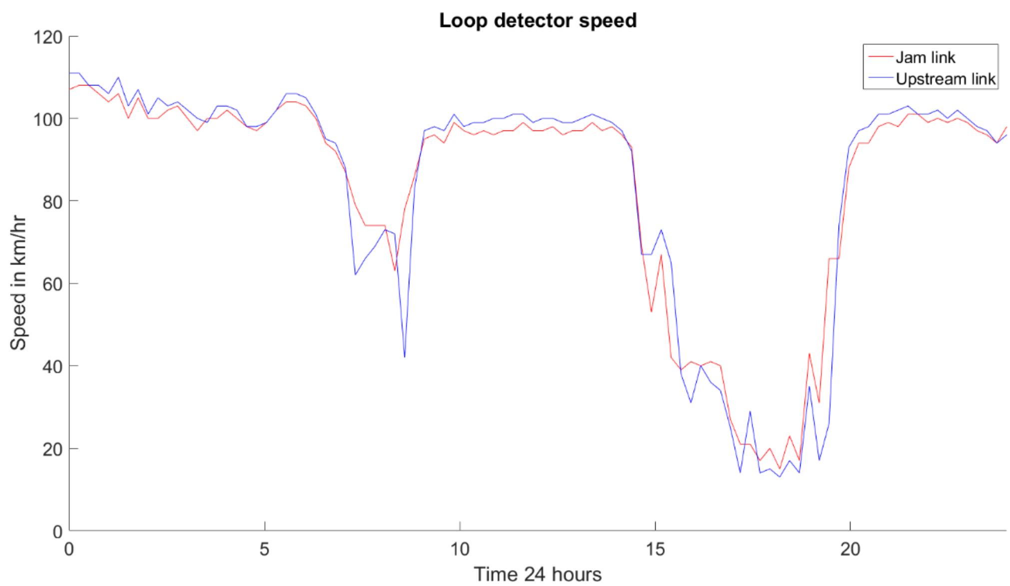

Figure 3-9 Loop detector mean speed measurement for one day with 15 minute interval.

Figure 3-10 and Figure 3-11 show the flow and density for both links during the day, flow in vehicles per hour and density in vehicles per kilometre. Between 00:00 and 07:00 am, the flow and density on the two links are very similar. This is because at this time of day vehicles travel in free flow phase and the delay between the two measurements is quite small compared to the aggregation level. To clarify consider an example: in Table 3-3 the loop detector output is listed for the time interval 06:15- 06:30 am for the upstream link and the jam link as plotted in Figure 3-9 and Figure 3-10. The delay is equal to the travel time between the two links in this case about one minute when the mean speed is

$100\ km/hr$. Thus considering the $\frac{3189}{4} = 797$ vehicles counted by the jam link detectors at the example time interval, $\frac{15-1}{15} * 797 = 744$ vehicles of which are also in the upstream link output at this time interval. Thus in the $15\ minutes$ between 06:15- 06:30 am $\pm 90\%$ of the vehicles that travel the upstream link, also travel the jam link.

LOOP DETECTOR OUTPUT FOR TIME INTERVAL 06:15- 06:30 AM

	Mean speed in km/hr	Mean flow in veh/hr
JAM LINK	$100\ km/hr$	3189
UPSTREAM LINK	$101\ km/hr$	3284

Table 3-3 Loop measurement example.

Overall the mean speed on the upstream link is higher than the mean speed on the jam link any time of day. The flow and density however differ depending on the time of day:

- Before the morning peak hour the flow and density on the upstream link and jam link are more or less equal. The highest flow rate is reached on the upstream link.
- Between the busy hours and after the evening peak hour, the flow and density on the upstream link are generally lower compared to the upstream link.

A common effect known as the capacity drop phenomenon (see Paragraph 2.3.1) causes a discontinuity in the capacity before the onset of congestion and after congestion has passed. These observations show how the capacity drop on the upstream link is larger than the capacity drop on the jam link which accounts for the difference in comparing flow and density on the links before or after congestion.
The size of the capacity drop has been studied to decrease with increased speed inside congestion [Yuan, 2014]. These observations support this theory as Figure 3-9 shows the lowest mean speed in congestion is measured on the upstream link.

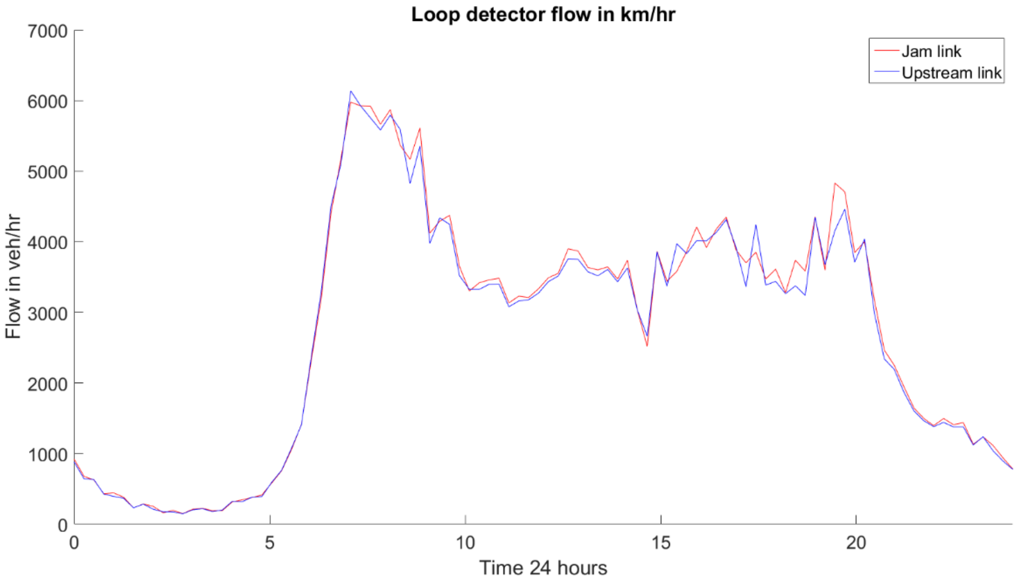

Figure 3-10 Loop detector flow measurement for one day with 15 minute interval.

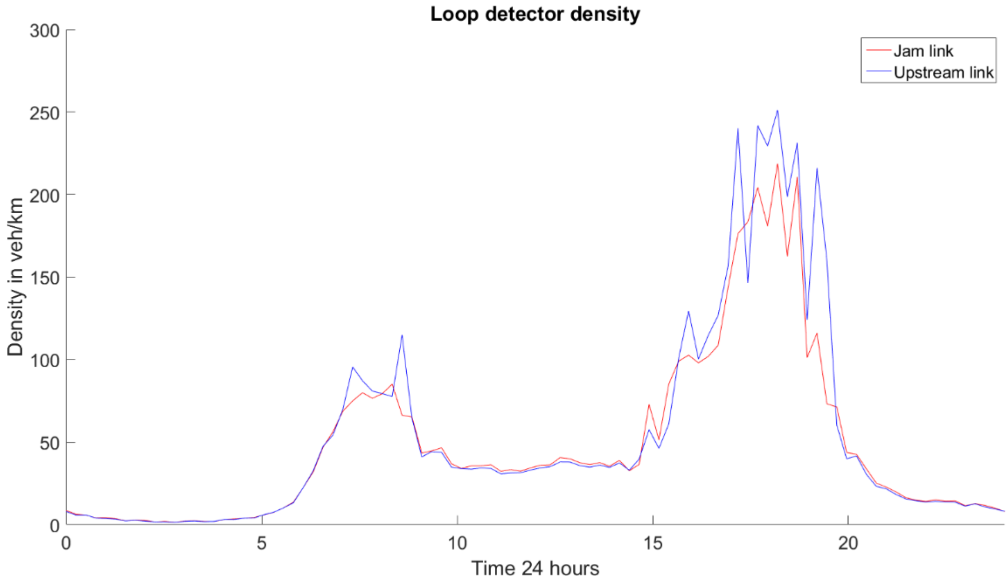

Figure 3-11 Loop detector density measurement for one day with 15 minute interval.

3.2.2 Validation

In the previous section of Paragraph 3.2 one day output data of the two experiment links are compared. It is found that outside busy hours:

- The mean speed on the jam link is lower than the mean speed on the upstream link.
- The capacity drop on the upstream link is larger than the capacity drop on the jam link.

To validate these observations the mean speed on the upstream link is compared to mean speed on the jam link at the same time instance. As mentioned the delay is small therefore it is assumed that this comparison is justified when mean speed and flow are sufficiently high.

Three times of day are specified, morning, midday and evening, where only hours outside busy hours are compared. Also flow values below 2000 veh/hr are disregarded and for the midday flow values below 3200 veh/hr are disregarded.

Mean speed comparison outside busy hours over 4 months $\boldsymbol{24\ hours = 96 * 15\ minutes}$		
Morning $\mathbf{03{:}30 - 06{:}30}\ \boldsymbol{am}$ $\boldsymbol{i = 15{:}26}$	$speed\ upstream\ link(i)\ \geq speed\ jam\ link(i)$	99%
Midday $\mathbf{01{:}00 - 03{:}00}\ \boldsymbol{pm}$ $\boldsymbol{i = 49{:}60}$	$speed\ upstream\ link(i)\ \geq speed\ jam\ link(i)$	93%
Evening $\mathbf{09{:}00 - 11{:}00}\ \boldsymbol{pm}$ $\boldsymbol{i = 81{:}92}$	$speed\ upstream\ link(i)\ \geq speed\ jam\ link(i)$	98%

Table 3-4 Comparing mean speed as a function of time.

In the same way as the mean speed Table 3-5 shows the flow on the upstream link compared to the flow on the jam link at the same time instance. The results show the difference in flow before the morning peak hour and after the morning peak hour. Where the flow before the morning peak hour is higher on the upstream link, between busy hours and after the evening peak hour the flow is mostly higher on the jam link.

Flow comparison outside busy hours over 4 months $24\ hours = 96 * 15\ minutes$		
Morning $\mathbf{03:30 - 06:30\ am}$ $\boldsymbol{i = 15:26}$	$flow\ upstream\ link(i)\ \geq flow\ jam\ link(i)$	77%
Midday $\mathbf{01:00 - 03:00\ pm}$ $\boldsymbol{i = 49:60}$	$flow\ upstream\ link(i)\ \geq flow\ jam\ link(i)$	11%
Evening $\mathbf{09:00 - 11:00\ pm}$ $\boldsymbol{i = 81:92}$	$flow\ upstream\ link(i)\ \geq flow\ jam\ link(i)$	13%

Table 3-5 Comparing flow as a function of time.

3.3 Macroscopic model fit

In this paragraph a macroscopic model is fitted to loop detector data from the A-13. With a macroscopic model important properties are estimated which are useful when making a simulation model as will be done in Chapter 4. The automatic fitting procedure proposed by Knoop and Daamen is used [Knoop 2014] for fitting the data.

3.3.1 Fitting procedure

The method consists of two steps. First a triangular fundamental diagram fit is done to separate the congested state from the free flowing traffic state. Next the fundamental diagram of Wu is used to fit the congested branch and the free flow branch separately [Wu 2002]. This method is shown to be robust for cases tested in real life, hence in case of noisy data, making it suitable for the purpose here. Figure 3-12 and Figure 3-13 show the results of the triangular fit for both the upstream link and the jam link.

3.3.2 Triangular fit for critical density estimation

The triangular model is defined by three parameters namely: the free flow speed, the critical density and the jam density. The free flow speed is the slope of the free flow branch as seen in Figure 3-12 and Figure 3-13. The critical density is the density where the flow is at its maximum which is equivalent to the estimated capacity. The jam density is the density where the flow of the congested branch is zero.

The wave speed or shockwave speed is the speed of the congested front moving upstream. For this fit the wave speed is fixed and therefore the jam density is fixed as the wave speed describes the slope of the congested branch. Since the wave speed is proven to be fairly constant for freeways and it hardly influences the capacity, it is fixed at $18\ km/hr$ which is the default wave speed value used for Wu's fundamental diagram [Wu 2002].

The free variables thus are free flow speed and the critical density. These variables are estimated by minimization of the error between the fit and the data. The results are listed in Table 3-6 below.

Regarding a robust fit a few assumptions are made. For the free flow data, speed measurements below $72\ km/hr$ are disregarded because this is considered an unlikely low mean speed outside peak hours. Therefore these points get weighted zero as can be seen in the figures. Measurements where the mean speed is below $36\ km/hr$ get a weight of 0.5, as shown by the yellow dots in Figure 3-12 and Figure 3-13. The reasoning behind this weighing factor is based on the fact that high density observations are unreliable. However totally disregarding these data points will not benefit a reliable fit therefore Knoop suggests a weighting factor for these data points.

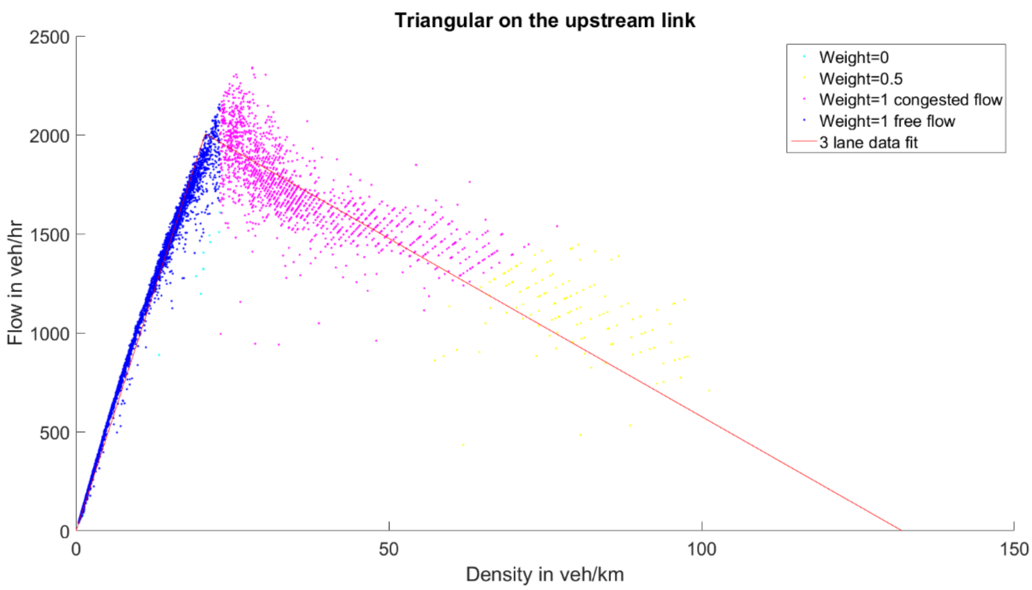

Figure 3-12 Triangular fit on the upstream link.

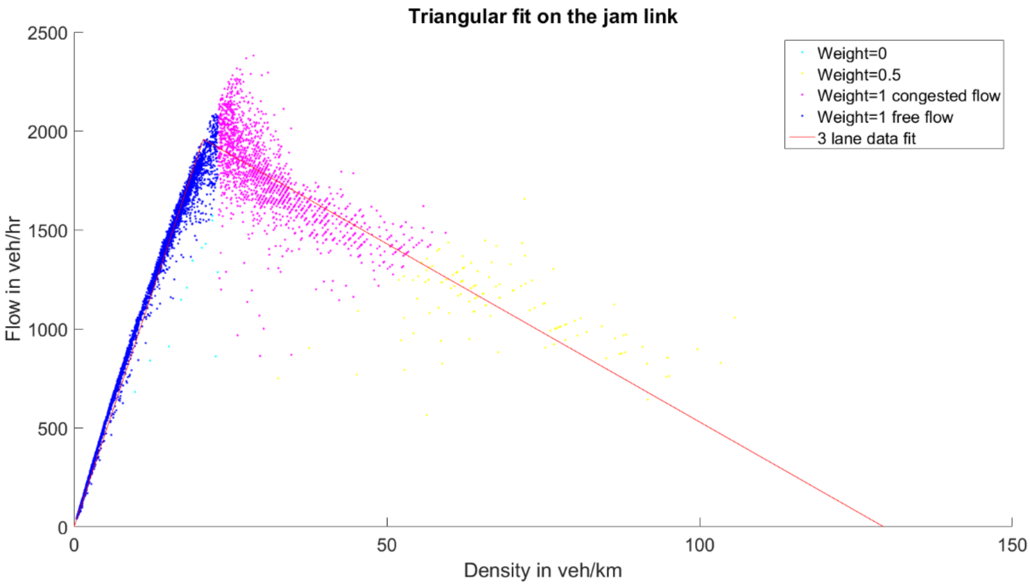

Figure 3-13 Triangular fit on the jam link.

	Upstream link	Jam link
Critical density with 95% confidence bounds	$\mathbf{20.63}\ \boldsymbol{veh/km}$ $(20.58, 20.69)\ veh/km$	$\mathbf{20.64}\ \boldsymbol{veh/km}$ $(20.59, 20.69)\ veh/km$
Free flow speed with 95% confidence bounds	$\mathbf{97.18}\ \boldsymbol{km/hr}$ $(96.97\ 97.39) km/hr$	$\mathbf{94.85}\ \boldsymbol{km/hr}$ $(94.64, 95.07) km/hr$
Capacity	$\mathbf{2005}\ \boldsymbol{veh/hr}$	$\mathbf{1958}\ \boldsymbol{veh/hr}$

Table 3-6 3 lane triangular fit results.

The purpose of the triangular fit is to estimate the critical density that separates the free flow branch from the congested branch of the fundamental diagram.

The results show how the estimated critical density is slightly lower on the upstream link. Besides the critical density, the free flow speed is a free variable as well which is higher on the upstream link, by multiplying the free speed and critical density the estimated capacity is given, see Table 3-6. The triangular fit suggests a 2% higher capacity on the upstream link. In the next paragraph a more realistic fit will be made for the free flow data and the congested data separately.

3.3.3 Free flow model estimation

In the previous section of Paragraph 3.3.2 the critical density is estimated via the triangular fit. The next step in fitting a robust macroscopic model to noisy detector data is separating the free flow data and the congested data in order to fit a more realistic model for both links. In this case Wu's model is fitted to the free flow branch and the congested branch separately. Wu's fundamental diagram is discontinuous, as the capacity is not equal to the flow discharge rate (see Paragraph 2.3). Wu's fundamental diagram is characterised by five parameters, being the free flow speed, wave speed, free flow capacity, queue discharge rate and jam density. Following the automatic fitting procedure as is suggested by Knoop and Daamen the free flow speed and the wave speed are fixed because they found the fitting is not very sensitive to the right values of these parameters [Knoop 2014]. In this case only the free flow speed is fixed as in the previous step it is found that fixing the wave speed at $18\ km/m$ is an overestimation for the upstream link, see Figure 3-12.
Also instead of disregarding data points within 10% below and 20% above the estimated critical density, here data points within 20% below and above are disregarded when fitting the free flow and congested branch. The reasoning behind this measure is to ensure a more robust fit when values close to the critical density are unreliable and this allows for an error in the critical density estimation.

Figure 3-14 and Figure 3-15 show the final product of the fitting procedure. The free flow branch is separated via the triangular fit. Next following Wu's fundamental diagram a free flow-, density flow relation is modelled with a linear least squares approximation.

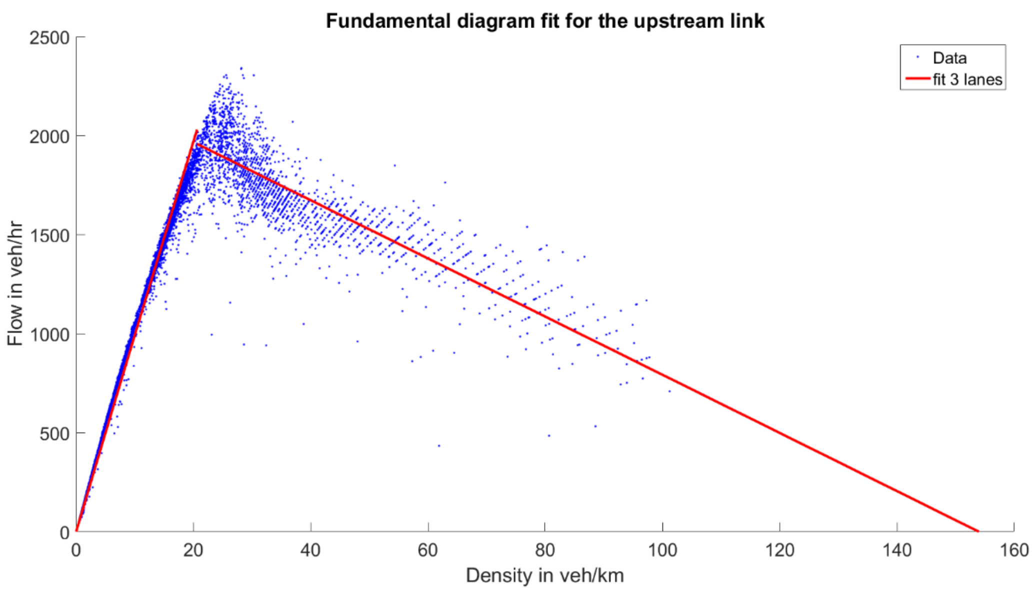

Figure 3-14 Fundamental diagram.

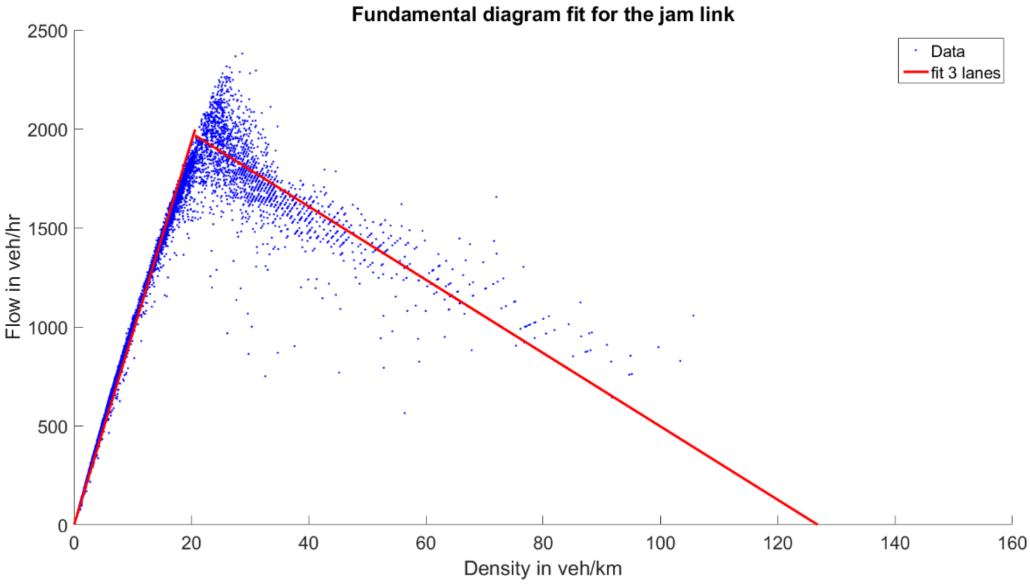

Figure 3-15 Fundamental diagram.

3.4 Conclusion

To conclude this chapter it is found that the pre queue capacity on the upstream link is higher than the pre queue capacity on the jam link. Therefore the jam link functions as a bottleneck.

However the capacity after congestion, the flow discharge rate, is lower on the upstream link compared to the jam link. Hence the capacity drop on the upstream link is larger than the capacity drop on the jam link as can be seen in Table 3-7.

Also it can be concluded that the observed traffic is more in a congested phase than it is in free flowing phase because between the morning and evening peak hour, 89% of the time the flow on the jam link is higher than the flow on the upstream link and after the evening peak hour 87% of the time the flow is higher on the jam link than on the upstream link.

	Upstream link	**Jam link**
Pre queue capacity	$2030\ veh/hr$	$1997\ veh/hr$
Queue Discharge rate	$1956\ veh/hr$	$1967\ veh/hr$
Capacity drop	$74\ veh/hr$	$30\ veh/hr$

Table 3-7 Fitting results.

3.5 Summary

In Chapter 3 a specific location on the A13 is studied where wide moving jams originate on this freeway. In Paragraph 3.3 a fundamental diagram is modelled for analysing purposes and to calibrate the Netlogo simulation model which will be the topic of Chapter 4.

In order to analyse the situation on the A13, loop detector data from two consecutive parts of the road are compared. The ‘’jam link’’ where the wide moving jam originates and the ‘’upstream link’’ where the wide moving jam travels upstream the traffic flow. Considering the jam direction the order is jam link and then upstream link, however the vehicles first pass the upstream link and then the jam link. Results from the fundamental diagram show a higher estimated free flow speed, capacity and capacity drop on the upstream link. In short, the jam link is a small bottleneck and therefore a wide moving jam will form when traffic conditions are unstable, when high speeds and density occur.

Time dependent data is compared since congested data is less reliable and it is difficult to separate from the free flow data via density. Results show how the capacity or pre queue capacity is only reached before the morning peak hour, the rest of the day the queue discharge rate is active. Therefore in this situation the capacity drop is critical.

4 Netlogo model

4.1 Introduction

In this chapter a microscopic traffic flow model is proposed and calibrated with the macroscopic free flow diagram as discussed in Chapter 0.

Netlogo is a modelling environment that allows for agent based models to be defined. Agent based models, often abbreviated as ABM models, have proven to be a very useful technique in predicting traffic flow in metropolitan areas and other areas. The power of this technology lies in the fact that the behaviour of a complex system can be simulated in which agents interact with each other and their environment using simple local rules. ABM is often used to simulate systems consisting of "behavioural" entities. In light of the purpose of this thesis, the ABM technique is especially suitable as it is aimed to relate vehicle properties (a microscopic characteristic) to aggregated data (a macroscopic relation).

NetLogo is particularly well suited for modelling complex systems developing over time. Modellers can give instructions to hundreds or thousands of "agents" all operating independently. This makes it possible to explore the connection between the micro-level behaviour of individuals and the macro-level patterns that emerge from their interaction.

4.2 Model objective and set up

The objective of the simulation model is to evaluate the macroscopic effects of speed composition on the road capacity and the capacity drop.

The A-13 is a three lane road but here is chosen to model the freeway with one lane. First of all, adding more lanes means a complex model since lane changing logic has to be established. Secondly, overtaking chances diminish when traffic is close to capacity and therefore the one lane simulation model can be calibrated to suit the free flow fundamental diagram.

Netlogo model parameters	value
Number of lanes	1
Number of patches	233
Patch length	7.5m

Table 4-1 Design parameters

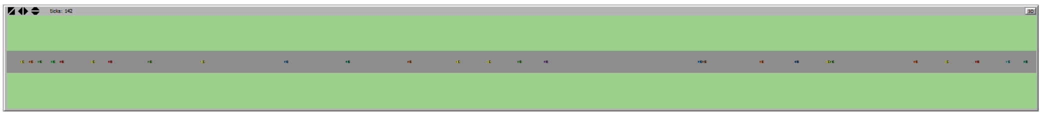

Figure 4-1 Road model segment total length is 1748 m.

The road is modelled by so called patches that are arranged in a grid. Each patch has a fixed location and represents a section of the road. The patch length is set to be $7.5\ m$ as per standard CA traffic simulation [Nagel, 2004]. The design behind the patch length is such that each vehicle occupies exactly one patch of road when it is stopped in a queue. It has been shown that this is a suitable patch length for this type of simulation, see [Nagel, 2004] for further reading. Together with the number of patches 233 the road length in meters is $1748\ m$, see Figure 4-1. The length of the jam link as discussed in Chapter 3 is $1750\ m$.

4.3 Model Variables

In this Paragraph each modelling variable is discussed with respect to the microscopic as well as the macroscopic behaviour. The next step in specifying the model is estimating the simulation time step. Subsequently the free speed composition is fixed and the acceleration/deceleration values are calibrated in Paragraph 4.4 where the simulation model is validated with the previously established fundamental diagram.

4.3.1 Simulation time step

The Netlogo model is a discrete time model. The accuracy and run time of such a model depends on the number of dynamic objects and the chosen simulation time interval or ''time slice''. Every simulation time step, all individual vehicles are updated in a random order. Per vehicle the action is determined based on a set of vehicle or driver dependent rules, for example:

''If the current speed is smaller than the free speed or desired speed: accelerate''

''If the current speed is equal to the free speed: remain speed''

And also rules for interaction:

''If the current speed in $patches/\Delta t$ *exceeds the distance to a preceding vehicle: decelerate''*

The smaller the simulation time interval Δt the higher the number of updates, and therefore the accuracy, increases with smaller time intervals and the runtime as well.

Besides accuracy and runtime the size of the simulation time step affects the speed and the steady state density and flow.

In Paragraphs 4.3.2, and 4.3.3 the relation between simulation time step and speed, density and flow are discussed.

4.3.2 Discrete speed

As both time and vehicle position are discrete parameters it follows that vehicle speed is a discrete function as well. Since the discrete vehicle position is set, the discrete speed depends only on the simulation time step size:

$$\Delta v = \frac{\Delta x}{\Delta t} \text{ in } km/hr$$

Equation 4-1

The step size of the discrete speed function is equal to the vehicle position step size, Δx divided by the simulation time step size, Δt. Figure 4-2 and Figure 4-3 show how the accuracy of speed relates to the size of the simulation time step. These figures show that when the time step increases, the accuracy of the speed increases.

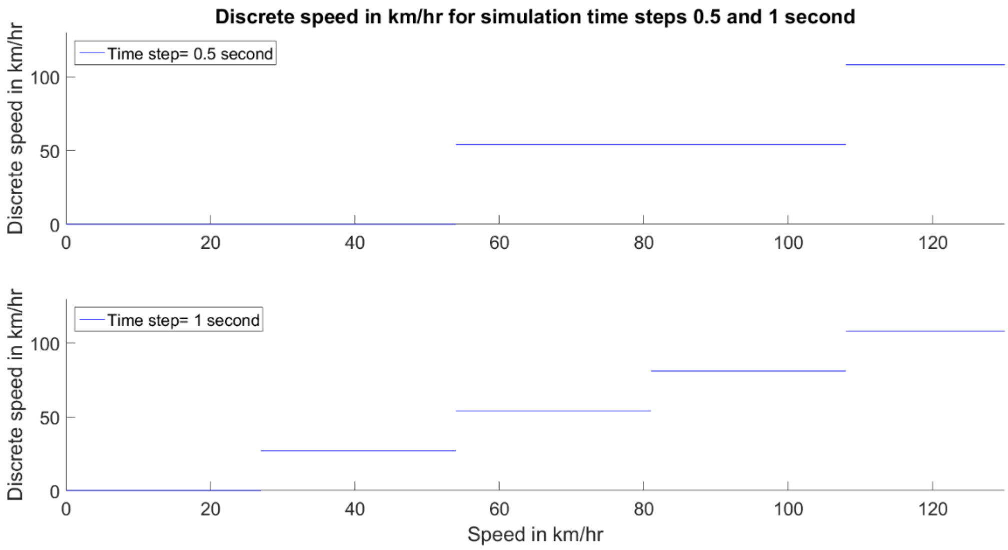

Figure 4-2 Discrete speed for simulation time step 0.5 and 1 second.

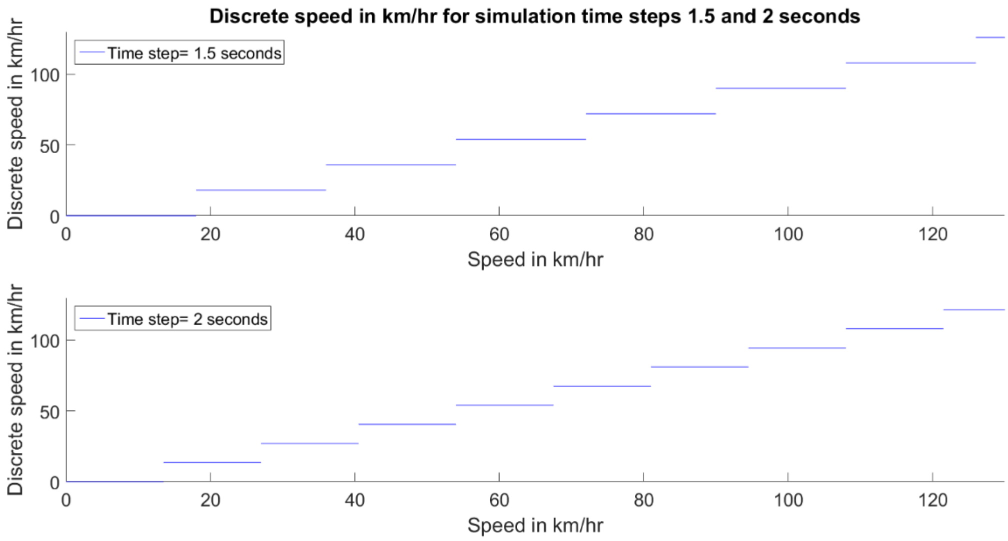

Figure 4-3 Discrete speed for simulation time step 1.5 and 2 seconds.

The following distance is defined as the distance a driver will ideally keep between the front bumper of his vehicle and the rear bumber of the vehicle in front of him. In The Netlogo model following distance is defined as the minimum distance between vehicles that will remain constant provided conditions downstream remain the same. Under these circumstances the speed is constant and the following distance depends only on the speed.

For example in Figure 4-4, looking at the green vehicle at $t = 0$, there are two simulation update possibilities since the update is in random vehicle order. Independent of the simulation update, at $t = 1$ the result is the same. Since possibility one shows the distance between the vehicles is minimal thus in this example the green vehicle is driving in following distance to the pink vehicle.

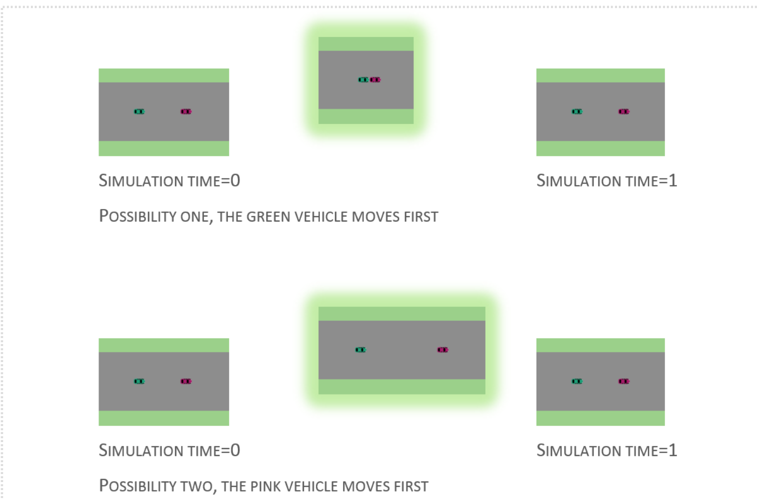

Figure 4-4 Illustration of the following distance. The speed does not depend on the simulation.

As the following distance depends only on speed in steady state the density can be calculated as a function of speed. Figure 4-5 and Figure 4-6 show the speed density relation in steady state for different simulation time steps. When the speed is $0\ km/hr$ hypothetically the density is at its maximum when all vehicles are bumper to bumper as the following distance is zero. From Figure 4-5 and Figure 4-6 it can be seen how, depending on the size of the simulation step, the steady state following distance and thus the density varies with speed. The smaller the simulation time step the smaller are the following distances which results in a higher density. When the speed is for example constant at $100\ km/hr$ the maximum density that can be reached is four times higher when the simulation time step is $\Delta t = 2\ s$ compared to $\Delta t = 0.5\ s$.

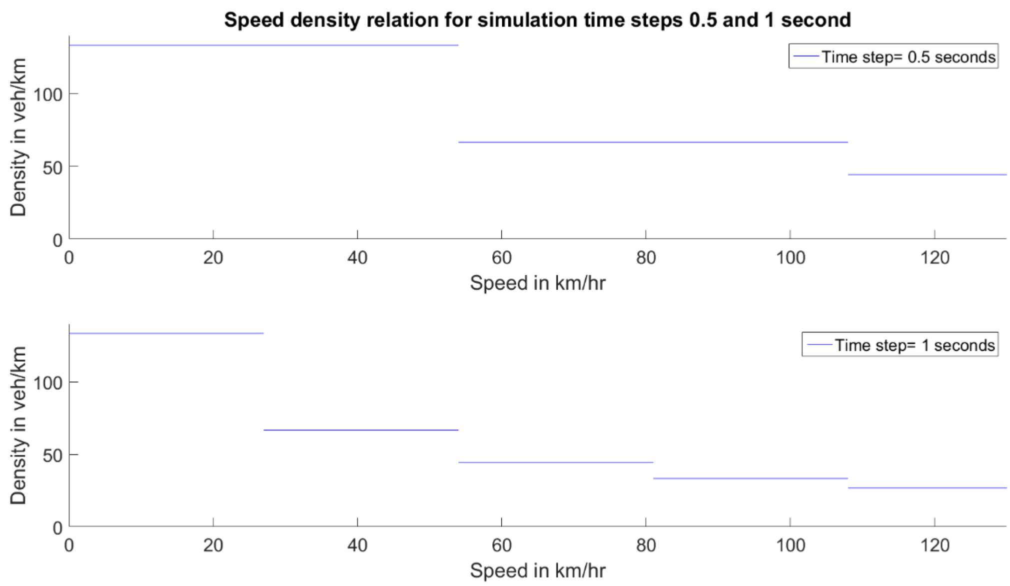

Figure 4-5 Steady state speed density relation for simulations time steps 0.5 and 1 second.

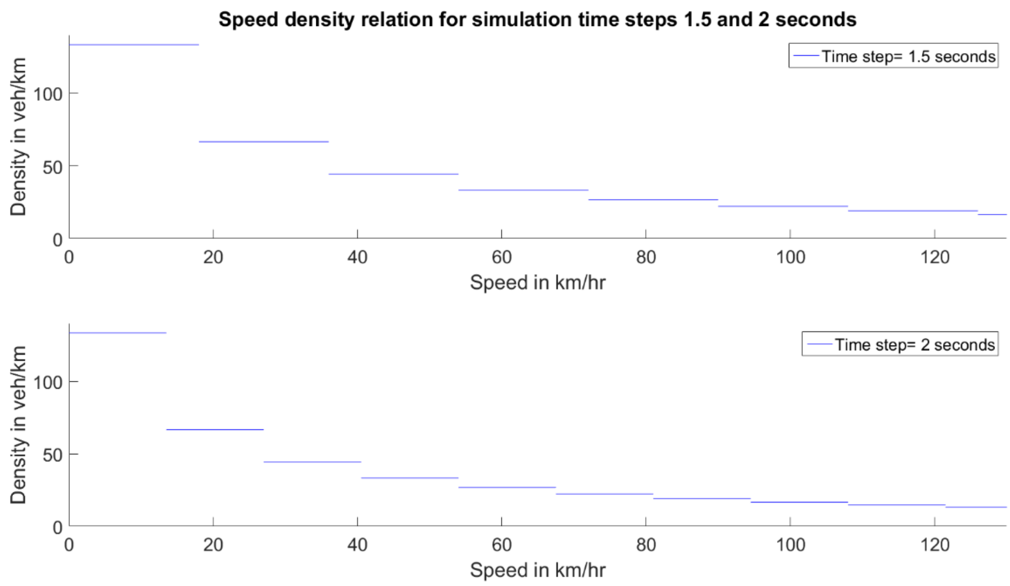

Figure 4-6 Steady state speed density relation for simulations time steps 1.5 and 2 seconds.

4.3.3 Steady state flow

In the previous paragraph steady state speed density relations were shown for various simulation time steps, Δt. Since the following distance depends only on speed in steady state, the flow in veh/hr can be found. Figure 4-7 and Figure 4-8 show the speed flow relations in steady state for different simulation time steps.

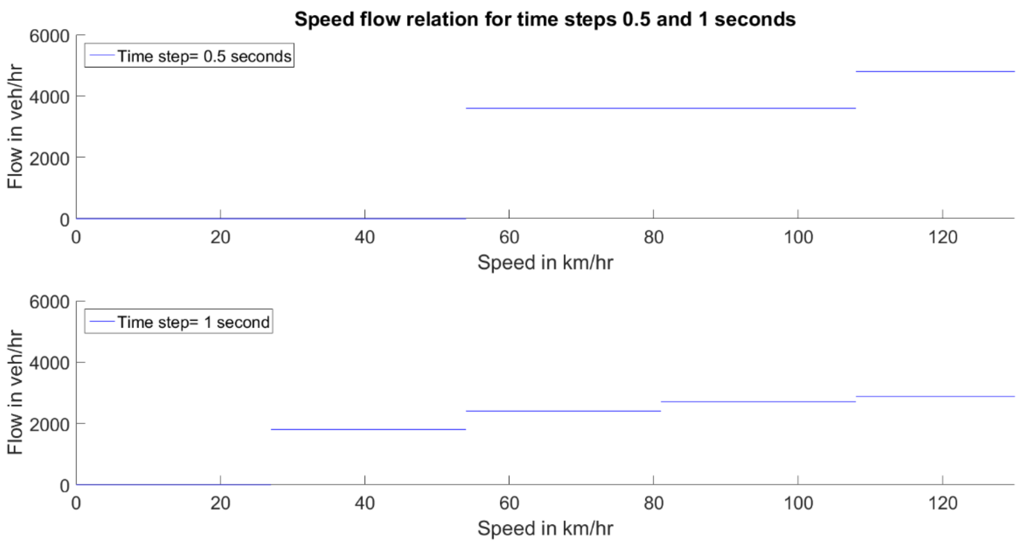

Figure 4-7 Steady state speed flow relation for simulations time steps 0.5 and 1 second.

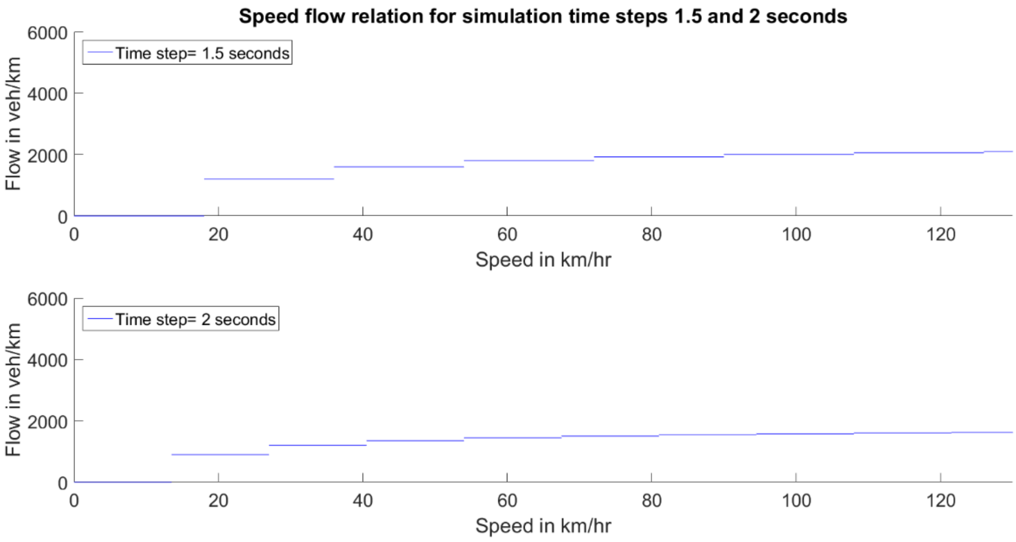

Figure 4-8 Steady state speed flow relation for simulations time steps 1.5 and 2 seconds.

Figure 4-7 and Figure 4-8 show how in steady state the speed is related to the flow for simulation time steps $0.5, 1, 1.5$ and 2 $seconds$. For each discrete speed, the maximum possible flow is plotted in vehicles per hour. In other words the figures show the road capacity as a function of speed. It can be seen how the simulation time step not only determines accuracy and runtime but also the capacity at a given speed.

4.3.4 Simulation time step and capacity

In Figure 4-9 the steady state speed flow relations are depicted for time steps 1 and 1.5 $seconds$ with the observations from the A13. It can be seen how the simulation time step determines the maximum flow that can be simulated at a certain speed. The steady state flow is the flow under ideal conditions where all vehicles behave the same, in real life the capacity is lower because vehicles do not behave in a uniform manner. As described, the first step in calibrating the miscroscopic Netlogo model is choosing the optimal simulation time step. In the previous paragraps of Chapter 4 it is shown how the simulation time affects the accuracy for each model parameter, besides the runtime.

Since the patch size is fixed (See Paragraph 4.2), the discrete speed is known given a certain time step. Furthermore because the steady state following distance only depends on speed, steady state flow and density are known as well.

Thus to simulate the capacity and free flow speed estimated for the A13, the simulation time step needs to be calibrated which is done in Paragraph 4.4. In Figure 4-9 it can be seen that the simulation time step is some value between 1 and 2 seconds because the highest flow observations from the A13 are in between the steady state speed flow relations for these two time steps.

There is a trade of between the time step and the accuracy of speed, density and flow. When the simulation time step is small the model is updated more which benefits the time accuracy however at the cost of speed density and flow accuracy as well as the runtime. When the simulation time step $\Delta t = 1\, seconds$, there is no difference in following distance when the speed is $85 km/hr$ or $100 km/hr$, see Figure 4-9.

On the other hand when the time step is higher, $\Delta t = 1.5\, seconds$, Figure 4-9 shows how the observations from the A13 exceed the steady state flow around capacity, when speed and flow on the A13 are highest. Meaning the simulation model will be unable to reach a high enough capacity when the speed is between $80 km/hr$ and $100 km/hr$. Also note here that the steady state values represent a hypothetical scenario where all vehicles behave the same, the actual simulation and the real life values lie below the steady state function.

Considering this, in Paragraph 4.4 the time step is chosen to be as large as possible which benefits the accuracy of speed while the flow is high enough to simulate the capacity estimated from the A13.

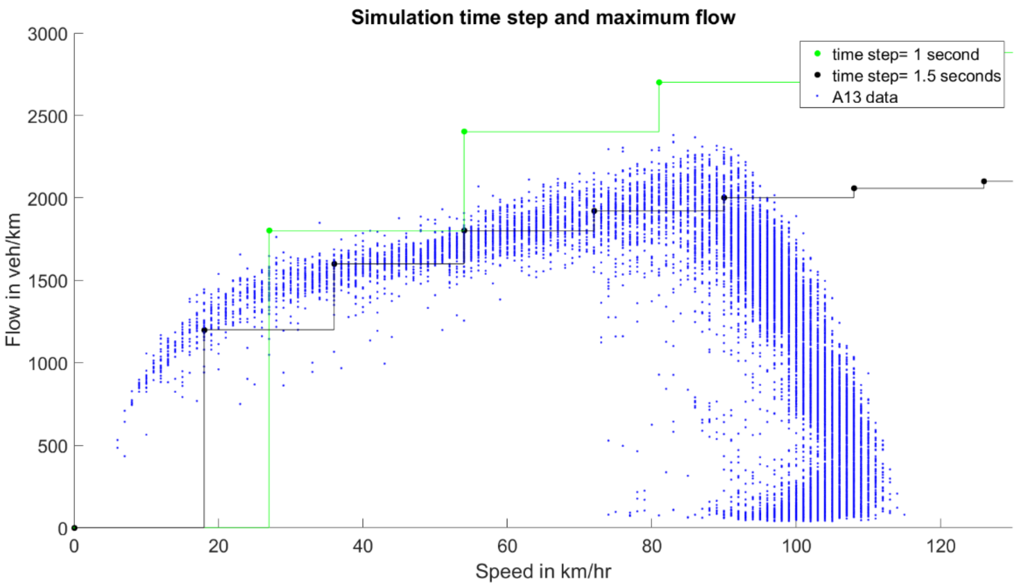

Figure 4-9 Steady state speed flow relations for time steps 1 and 1.5 seconds.

4.3.5 Free or desired speed

The free speed or desired speed is the speed a driver will choose to travel when there is no interference with other vehicles. As mentioned in the previous section, see Paragraph 4.3.2, the free speed is a discrete parameter defined in $patches/\ discrete\ time\ step$.

The general idea is that large relative speeds go together with lane changes and overtaking.

In [Hoogendoorn 2005] detailed vehicle data has been used to determine a relation between the headway and relative speeds and the share of vehicles that are constrained under these conditions, for two-lane rural roads in the Netherlands. Even more so when there are no overtaking chances, the larger the free speed distribution the larger the share of constrained vehicles. In this thesis the effect of increasing the ratio of fast-/slow vehicles on capacity is simulated. The size of the free speed distribution is kept constant while the percentage of fast and slow vehicles is varied.

4.3.6 Travel demand frequency

In this thesis the travel demand consists of two parts, the travel demand frequency and a travel demand rule. The travel demand rule determines the minimal gap between a vehicle wanting to enter the road section and its *possible* predecessor. This variable determines the specific shape of the free flow curve and is one of the calibration variables and therefore will be discussed in Paragraph 4.4. As opposed to the travel demand minimal gap, the travel demand frequency does not depend on speed. The frequency gives the number of vehicles that want to enter the road independent of the density on the road or if the certain vehicle is allowed to actually enter the road segment. The frequency variable f is a percentage that represents the probability of a vehicle wanting to enter the road section per time step Δt: $P(X = 1)$. With X a discrete random variable in vehicle per simulation time step with sample space Ω={0,1}.

$$P(X = 1) = \frac{f}{100} \text{ for each sample.}$$

Equation 4-2

$$0 \leq f \leq 100$$

Equation 4-3

4.3.7 Acceleration/ deceleration

Acceleration and deceleration are defined as the maximum difference in speed per simulation time step in $patches/\ simulation\ time\ step$. In literature it is often discussed how the acceleration/ deceleration behaviour is largely responsible for the capacity drop phenomenon, (See Paragraph 2.3.1).

Especially vehicle acceleration holds a close relation to the critical density and capacity and therefore this variable is a calibration variable in Paragraph 4.4. The deceleration will be set to $7m/s^2$ as often seen in this type of simulation.

4.4 Calibration

In this paragraph the remaining model variables simulation time step, free speed, the minimal entering gap and maximum acceleration are calibrated. These four variables determine the specific shape of the free flow branch of the fundamental diagram. The fundamental relation of Figure 3-15 shows how the steepness of the density flow curve decreases when density increases. The magnitude of this decrease depends on the overtaking opportunities and thus the number of lanes. In this thesis it is assumed one lane can be used to estimate the modelled free flow branch of the fundamental diagram in Chapter 3. Instead of using lane changing logic, the minimal entering gap is used to model the critical density and capacity on the A13. In the next paragraph, 4.4.1, the simulation time step is calibrated which determines the maximum capacity and the accuracy of the free speed that will be possible to simulate. The calibration of the remaining variables is done as follows: first the free speed and initial gap are fixed. Next appropriate ranges for each calibration variable are established. Finally the calibration is done by minimizing the error between the free flow curve and the estimated critical density and capacity from Paragraph 3.3.3.

4.4.1 Time step calibration

As described in Paragraph 4.3.4 the appropriate simulation time step is a value between $\Delta t = 1$ and $\Delta t = 1.5$ seconds. The goal is to choose a simulation time step that is higher than $\Delta t = 1$ second to benefit speed accuracy but smaller than $\Delta t = 1.5$ seconds in order to be able to simulated the highest flow observations from the A13. Figure 4-10 shows the figure from Paragraph 4.3.4 with the calibrated simulation time step $\Delta t = 1.14$ seconds.

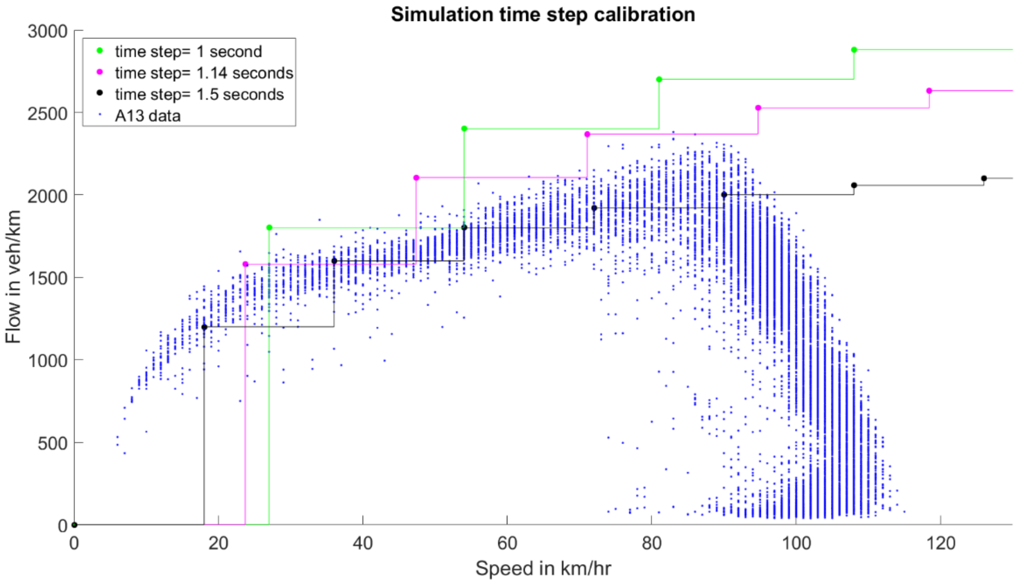

Figure 4-10 Steady state speed flow relations for time steps 1, 1.14 and 1.5 seconds.

4.4.2 Fixing free speed and initial gap

To calibrate the microscopic simulation model with the free flow relation found in Paragraph 3.3.3, first the assumption is made that on average vehicles can be divided into two groups, the slow vehicles and the fast vehicles. As can be seen in Figure 4-10 and Figure 4-11, the chosen simulation time step fixes the discrete speed and thus the options to choose the free speed of the slow and fast vehicles. Figure 4-12 shows the assigned free speed to the slow and fast vehicles together with the free flow branch of the A13 fundamental diagram.

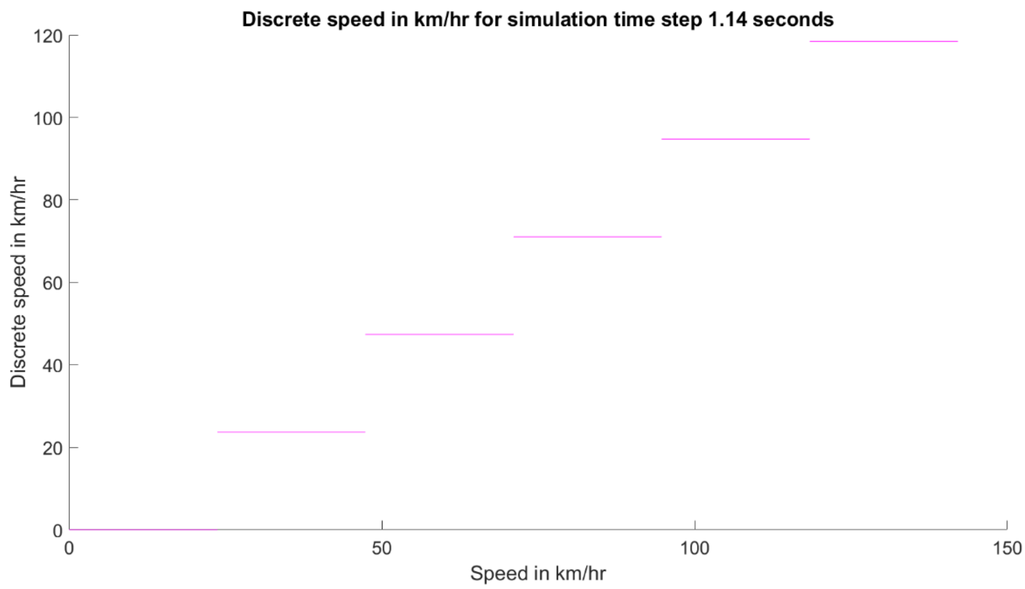

Figure 4-11 Discrete speed for simulation time step 1.14 seconds.

Figure 4-12 shows the fundamental diagram free flow branches from Paragraph 3.3.3 with constant speed slopes 95 km/hr, in green and 118 km/hr in red, see Figure 4-11 for the discrete speed intervals. When the density is low the estimated free speed lies between the two constant speed slopes, see Figure 4-12.

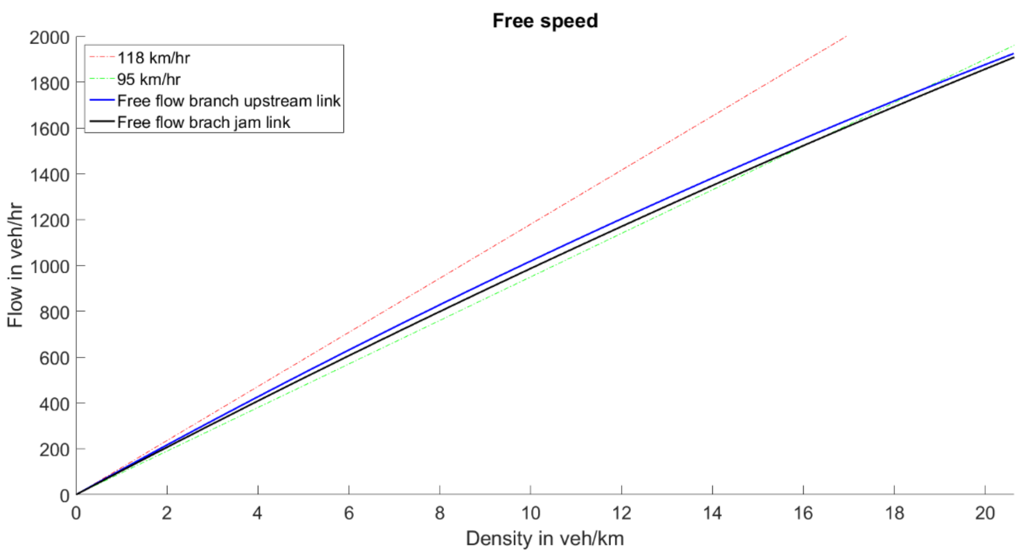

Figure 4-12 The free flow branches for the upstream and jam link from the fundamental diagram, see Paragraph 3.4.3.

The initial gap is the travel demand rule introduced in Paragraph 4.3.6. Together with the frequency, the initial gap determines the travel demand. A vehicle will only be allowed to enter the road section given a certain minimum free space, measured in patches, defined as the initial gap.

As well as the following distance this minimal initial gap depends on vehicle speed. For this reason the initial gap is fixed with the free speed, the initial gap is set separately for the low free speed and the higher free speed.

Figure 4-13 and Figure 4-14 show how the initial gap affects the density and flow for respectively the fast and slow vehicles. Each figure shows simulations where speed, acceleration and deceleration are constant and the simulation length is fifteen minutes. For 10 frequencies (equally spaced between 5 and 100) 100 simulation results are plotted.

Initial gap calibration for free speed 118 km/hr

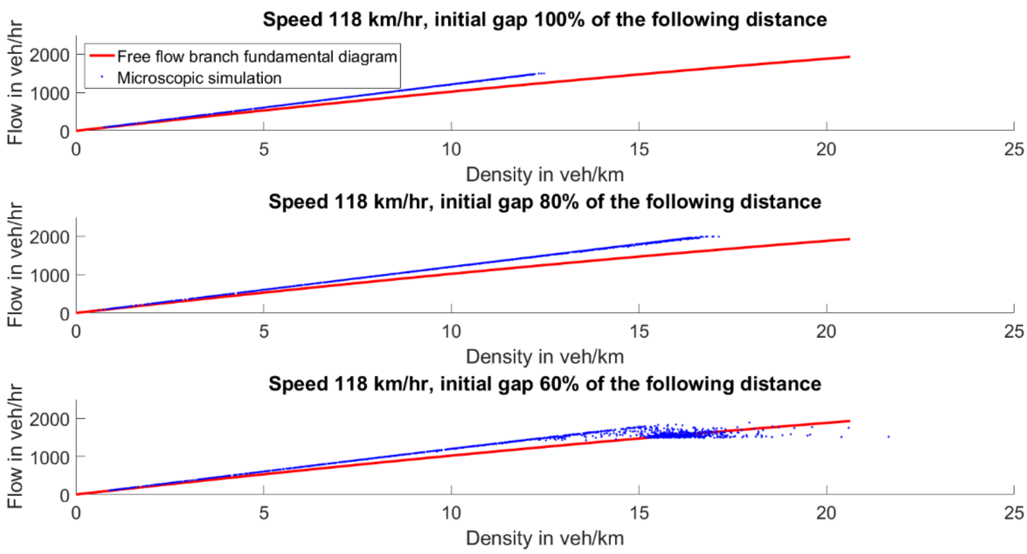

Figure 4-13 Acceleration is 3.3 〖m/s〗^2 and the initial gap is given in relation to the following distance. The solid red curve is the estimated free flow curve from the upstream link from Paragraph 3.4.3.

Initial gap calibration for free speed 95 km/hr

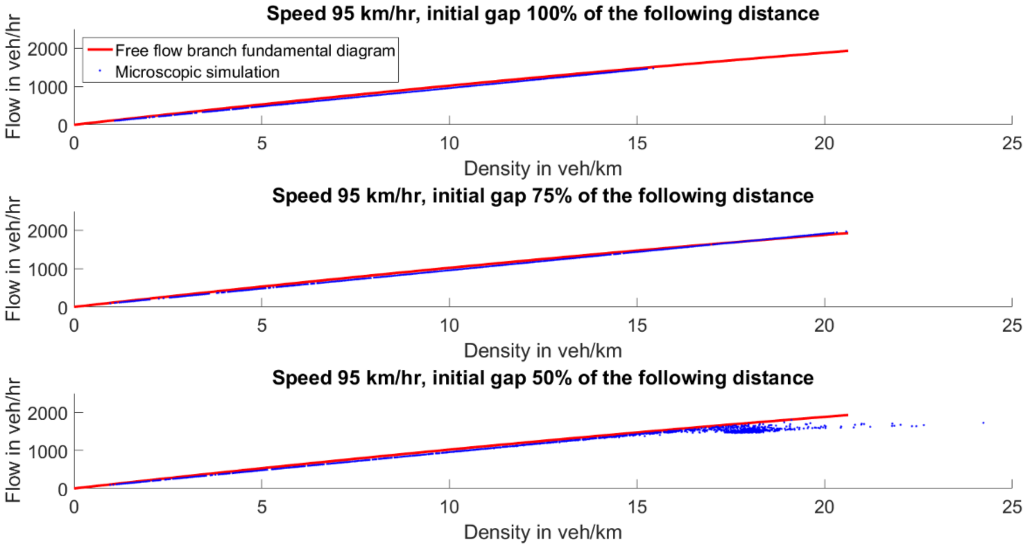

Figure 4-14 Acceleration is 3.3 〖m/s〗^2 and the initial gap is given in relation to the following distance. The solid red curve is the estimated free flow curve from the upstream link from Paragraph 3.4.3.

For both constant free speeds the optimal initial gap is when the highest flow is reached, see Figure 4-13 and Figure 4-14. The optimal initial gap that follows for a free speed of 95 km/hr is the initial gap equal to 75% of the following distance at this speed which is equal to 22.5 m. For a free speed of 118 km/hr the initial gap is 30 m or 80% of the following distance at this speed. The free speed is now fixed with the initial gap and the resulting calibration variable is the ratio between: vehicles with free speed 95 km/hr and initial gap 22.5 m and vehicles with free speed 118 km/hr and initial gap 30 m. In Table 4-2 and Table 4-3 the results from the simulations in Figure 4-13 and Figure 4-14are listed when there is no capacity drop.

Free speed 118 km/hr		Maximum flow	Density at capacity
	Initial gap 37.5 m, 100% of the following distance.	1496 veh/hr	12 veh/km
	Initial gap 30 m, 80% of the following distance.	1996 veh/hr	17 veh/km

Table 4-2

Free speed 95 km/hr	Maximum flow	Density at capacity
Initial gap $30\ m$, 100% of the following distance.	$1476\ veh/hr$	$15\ veh/km$
Initial gap $22.5\ m$, 75% of the following distance.	$1968\ veh/hr$	$21\ veh/km$

Table 4-3

4.4.3 Calibration result

The model calibration is done in two steps. First the ratio between the high and low speed is calibrated for only the low density region by minimizing the error between the simulation and the free flow branch of the fundamental diagram from Paragraph 3.3.3.
Next the maximum acceleration is calibrated by minimizing the error between the simulation capacity and the free flow capacity as modelled in Paragraph 3.3.3. Table 4-4 shows the results of the calibration. For the calibration of the ratio high to low free speed the root-mean-squared error (RMSE) is calculated for densities below 15 veh/hr. Table 4-4 shows the RMSE for 9000 samples.

Model variables		Goodness of fit
Free speed ratio $95\ km/hr$ / $118\ km/hr$	$50/50$	RMSE: $759\ veh/hr$
Maximum acceleration in m/s^2	3.7	RMSE: 7.44 veh/hr

Table 4-4 Model calibration results.

The simulation capacity is calculated as follows:
To find the free flow capacity from the simulation data, the critical frequency needs to be determined, this is the frequency where the boundary between the free flow phase and the congested phase is.
The estimated maximum flow from the least squares fit for all free flow frequencies is defined as the capacity.
One simulation set consists of 20 times 900 simulations, for all 20 frequencies from $f = 5\%$ to $f = 100\%$, 900 simulations are done with each a duration of 15 minutes.

Starting with $x = 75\%$ all data upto where the frequency is 75% is fitted via least squares, giving an estimated maximum flow, $fmax_{75\%}$ and density, $d_{75\%}$. Next a 5% higher frequency is added to the data and again a least squares fit is done, when the resulting estimated flow, at $d_{75\%}$ is smaller than the estimated maximum flow $fmax_{75\%}$, $f = 75\%$ is the critical frequency and $d_{75\%}$ is $d_{critical}$, see Equation 4-4, else the same procedure is repeated for $f = 80\%$.

$$LSfit_{f=5:f_{critical}}(d_{critical}) > LSfit_{f=5:f_{critical+5\%}}(d_{critical})$$

Equation 4-4 Where $\mathrm{d}_{critical}$ is the maximum estimated density for $LSfit_{f=5:f_{critical}}$

The critical frequency is determined by comparing the least squares estimated maximum flow for frequencies $f = (5\%\ f_x)$ with the least squares estimated flow for frequencies $f = (5\%\ f_{x+5\%})$ at the same density.

Figure 4-15 shows the result of the calibration. The plot on the left shows the microscopic simulation model free flow branch and the capacity drop. The plot on the right shows the microscopic simulation model free flow branch together with the free flow branch from the fundamental diagram, see 3.3.3. The capacity drop is calculated by:

$$LSfit_{f=5:critical+5\%}(d_{critical})$$

Equation 4-5

Figure 4-15 shows the result of the least squares estimation $LSfit_{f=5:f_{critical}}$.

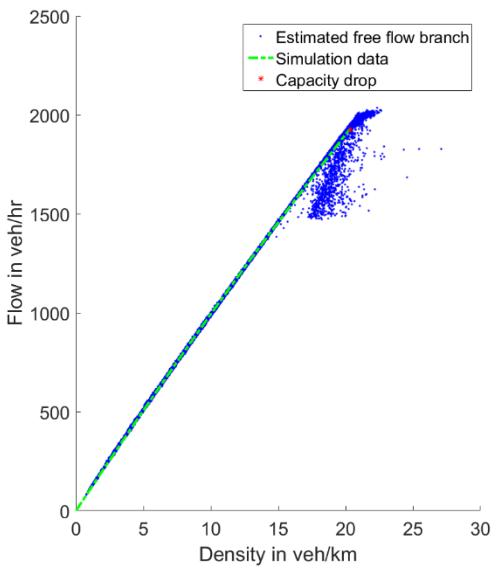

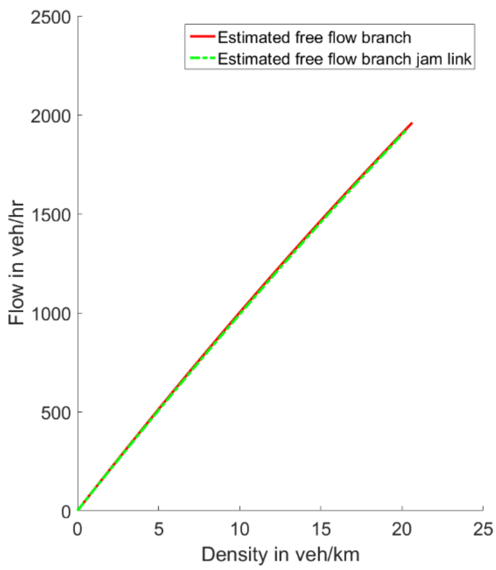

Figure 4-15 Calibration result.

% of vehicles moving at low speed	Critical density in veh/km	Critical frequency f	Free flow capacity in veh/hr	Flow discharge rate in veh/hr	Capacity drop in %	Estimated free flow speed in km/hr
50%	20.3	80%	1930	1906	1%	103.6

Table 4-5

5 Simulation

5.1 Introduction

Since the aim of this thesis is to study the effect of encouraging vehicles to maintain or even increase their speed, this paragraph entails the effect of the percentage of slow vehicles on the capacity.

In Chapter 4 a microscopic simulation model is proposed that will be used to simulate the capacity, capacity drop and the critical density for different free speed combinations. In Paragraph 5.2 the jam link will be simulated. The following paragraph will discuss different levels of user compliancy to the measure of decreasing the percentage of slow vehicles.

5.2 Upstream link and jam link

In Chapter 0 it was found that a small decrease in free flow speed can create a bottleneck. Another conclusion was made based on the fundamental diagram that the capacity drop on the upstream link is typically higher than the capacity drop on the jam link.

The microscopic model is calibrated in Chapter 4 on the jam link with a ratio of fast to slow vehicles of $50\%/50\%$. In the next paragraph simulations are done where the percentage of fast and slow vehicles is varied. The results show the effect of free speed ratio on the capacity and critical density.

5.3 Free speed composition

In this paragraph two scenarios are evaluated: one where the percentage of slow vehicles with a free speed of 95 km/hr exceeds the percentage of high speed vehicles with a free speed of 118 km/hr and the other way around.

For frequencies between $(5\% \; 100\%)$ in steps of 5%, thus for 20 frequencies, 900 simulations are carried out thus each plot shows $18{,}000$ simulations each with a length of $15 \; minutes$. Figure 5-1 shows the results of simulations where the amount of slow vehicles (with free speed $95 \; km/hr$) is lower than the amount of fast vehicles (with free speed $118 \; km/hr$). The percentage of slow vehicles decreases in each plot, ranging from 40% in the left picture to 20% in the right picture. In each plot the results of the simulations are shown together with the least squares free flow branch fit. The fit results are listed in Table 5-1.

Decreasing the percentage of slow vehicles clearly improves flow, the estimated capacity increases as the percentage of slow vehicles decreases. Also the critical frequency increases which means less congestion.

It can be seen how no matter the amount of simulations where congestion occurs, the distribution of flow and density does not vary much. As the percentage of slow vehicles goes down, the amount of simulations where congestion occurs goes down while the pattern of congested simulations remains constant. Thus the flow discharge rate is more or less constant.

The critical density goes up as the percentage of slow vehicles is decreased because congestion is less likely to occur.

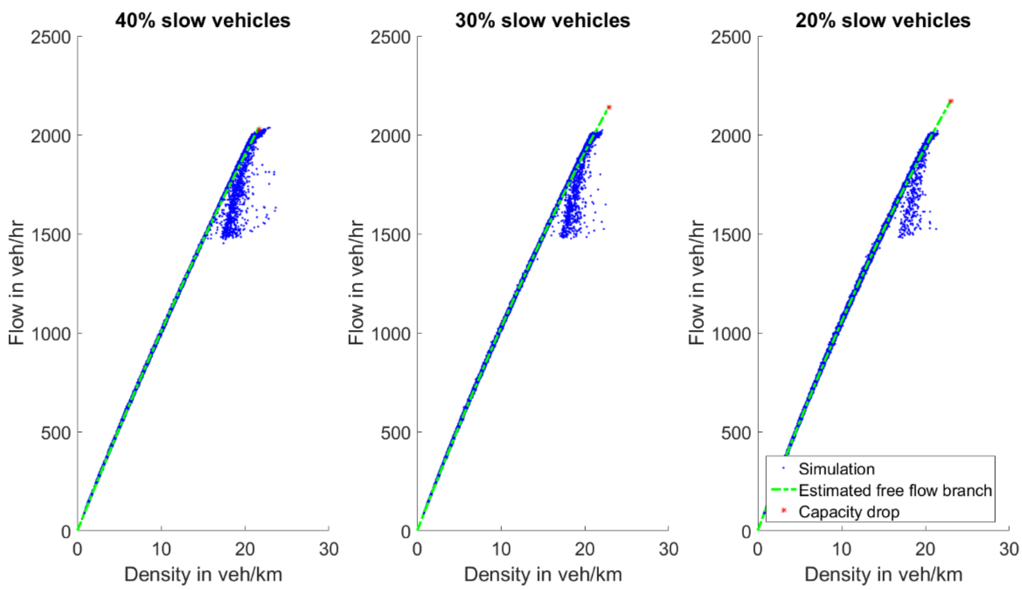

Figure 5-1 Estimated free flow branch for lowered percentage of slow vehicles.

% of vehicles moving at low speed	Critical density in veh/km	Critical frequency f	Free flow capacity in veh/hr	Flow discharge rate in veh/hr	Capacity drop in %	Estimated free flow speed in km/hr
40%	21.7	85%	2045	2027	1%	106
30%	22.9	90%	2146	2144	0%	110
20%	23.0	95%	2172	2169	0%	114

Table 5-1

In the next figure the results of the simulations are shown where the percentage of slow vehicles with a free speed 95 km/hr exceeds the percentage of vehicles with a free speed of 118 km/hr. The amount of vehicles with free speed 95 km/hr increases in each plot from 60% in the left picture to 80% in the right picture. Figure 5-2 and Table 5-2 respectively show the result of the simulations and the estimated free flow branch and the results of the least squares fit.

It can be seen that when the percentage of slow vehicles increases, the estimated capacity decreases. As opposed to the previous case shown in Figure 5-1, the estimated critical frequency is constant.

The estimated critical density goes down while congestion is less likely to occur because the congestion pattern changes. In Figure 5-2 it can be seen that the number of simulations in which congestion occurs decreases from left to right, however the level of congestion increases.

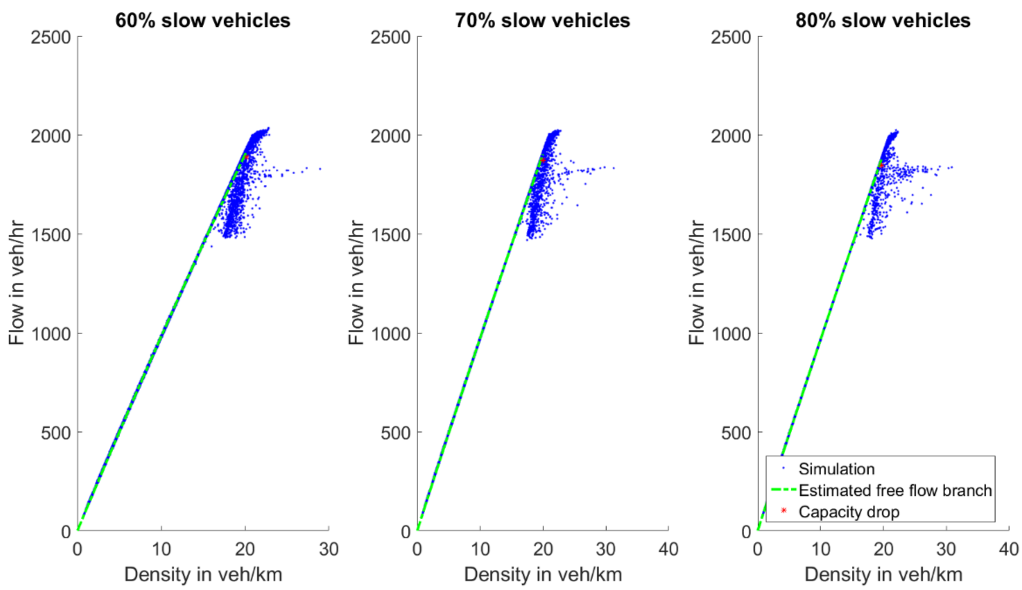

Figure 5-2 Estimated free flow branch for increased percentage of slow vehicles.

% of vehicles moving at low speed	Critical density in veh/km	Critical frequency f	Free flow capacity in veh/hr	Flow discharge rate in veh/hr	Capacity drop in %	Estimated free flow speed in km/hr
60%	20.2	80%	1915	1887	1%	101
70%	20	80%	1903	1870	2%	100
80%	19.2	80%	1876	1846	2%	97

Table 5-2

5.4 Conclusion

It is shown that a more uniform free speed decreases the number of simulations in which congestion occurs. This can be seen for both the case in which the percentage of low vehicles exceeds the percentage of fast vehicles and the other way around. However, while the number of simulations in which a congestion occurs decreases, the level of congestion increases in the scenario where the percentage of slow vehicles exceeds the percentage of fast vehicles. As a result the estimated critical density decreases even though the number of simulations where congestion occurs goes down.

In the scenario where the percentage of fast vehicles exceeds the percentage of slow vehicles the level of congestion stays more or less constant. Therefore critical density and capacity increase as the percentage of slow vehicles goes down.

6 Conclusion & Recommendations

The aim of this thesis is to investigate whether stimulating road participants to increase their free speed can prevent wide moving jams. The results of the analysis first of all show that uniform free speed improves traffic stability. This holds for both scenarios, whether the vehicle free speed is mainly high or low; a more uniform free speed decreases the occurrence of congestion for all simulations. Secondly, the ratio between fast and slow vehicles affects the level of congestion. Simulation results show how a free speed ratio with a majority of fast vehicles is preferred to the reversed case where the majority is slow because the level of congestion stays reasonably constant as opposed to an increased level of congestion.

These results confirm that encouraging drivers to retain or even increase their speed at locations where slow moving jams tend to form will decrease the likeliness of congestion and decrease the capacity drop.

In this thesis, detector loop data is used with a relatively high aggregation level of 15 minutes. A recommendation for further research is to analyse individual speed measurements or detector loop data with a smaller aggregation level to get better insight into the distribution of free speed. This has proven not to be a straightforward task since fast vehicles have a higher chance of experiencing constraints than slow vehicles. However, simulations with different free speed levels should be done to validate the results in this thesis. The composition of free speed affects both the capacity and the capacity drop. In this thesis the free speed range is kept constant. Simulations can be carried out for different free speed ranges to see whether the results found in this thesis hold for smaller or larger relative speeds.

In this thesis the A13 is modelled as one lane, to this end a small road section is taken and lane changing behaviour is simulated by controlling the entrance of the road section. Although the simulation model is calibrated with macroscopic relations from the A13 it should be checked if microscopic properties like lane occupation are realistic. The functionality should be verified for different road occupation scenarios by comparison of simulation results with a multi-lane model.

An important factor in effectiveness of the proposed measure depends on user compliancy. In this thesis it is proposed to encourage drivers to retain or increase their speed by making use of the smiley sign. It should be investigated whether the smiley sign is indeed the right sign to reach this goal or if a different sign would be more effective.

References

Akçelik, R. 2008. The relation between Capacity and Driver Behaviour. Paper presented at the TRB National Roundabout Conference. Kansas City USA.

Dijker, T., Bovy, P., Vermijs, R. 1998. Car-following under congested conditions: Empirical findings. Transportation Research Record 1644.

Edie, L. 1965. Discussion of traffic stream measurements and definitions. 2nd International Symposium On the Theory of Traffic Flow, Paris.

Federal Highway Administration (FHWA), 2012. Recurring Traffic Bottlenecks: A Primer-Focus on Low-Cost Operational Improvements. U.S. Department of Transportation Federal Highway Administration Office of Operations. www.fhwa.dot.gov FHWA-HOP-12-012.

Greenshields, B. 1934. A study of traffic capacity. In “Highway Research Board Proc.” Traffic Bureau, Ohio State Highway Department.

Hegyi, A. 2004. Model Predictive Control for Integrating Traffic Control Measures. TRAIL Thesis Series T2004/2, The Netherlands TRAIL Research School.

Hegyi, A. , Hoogendoorn, S.P, Schreuder, M., Stoelhorst, H., Viti, F., 2008. SPECIALIST: A dynamic speed limit control algorithm based on shock wave theory. Department of Transport & Planning, Faculty of Civil Engineering and Geosciences, TU Delft. 11th International IEEE Conference on Intelligent Transportation Systems.

Hegyi, A. 2013. Roadside-cooperative speed control algorithm to resolve moving jams (COSCAL v2). Tech. Rep. TU Delft sponsoring organization: Rijkswaterstaat – Water, Verkeer en Leefomgeving.

Hegyi, A., Weg, van de G.S, 2014. Spoken bestaan niet. Journal article. NM Magazine, 9 (1).

Hoogendoorn, S.P., Bovy, P.H.L. 2001. State-of-the-art of Vehicular Traffic Flow Modelling. Special Issue on Road Traffic Modelling and Control of the Journal of System and Control Engineering, Faculty of Civil Engineering and Geosciences, Delft University of Technology.

Hoogendoorn, S.P., Hegeman, G.& Dijker, T. 2004. Traffic Flow Theory and Simulation. Reader vk4821, Faculty of Civil Engineering and Geosciences, Delft University of Technology.

Hoogendoorn, P. 2005. Vehicle-type and Lane-Specific Free Speed Distributions on Motorways. TRB Annual Meeting. Delft University of Technology, Faculty of Civil Engineering and Geosciences.

Kerner, B. S. 2003. Three-phase traffic theory and highway capacity. Daimler Chrysler AG, RIC/TS, T729, 70546 Stuttgart, Germany.

Kerner, B. S.,Rehborn, H., et al. 2004. Recognition and tracking of spatial temporal congested traffic patterns on freeways. Transportation Research Part C.

Knoop, V.L., Duret, A., Buisson, C., Arem. B. 2010. Lane Distribution of Traffic Near Merging Zones Influence of variable speed limits. Faculty of Civil Engineering and Geosciences, Delft University of Technology.

Knoop, V.L., Daamen, W. 2014. Automatic fitting procedure for the fundamental diagram. Delft University of Technology Transport & Planning The Netherlands.

Leeuwen, A.S. van 2011. Static Traffic Assignment with Queuing. Master Thesis Applied Mathematics, University of Twente.

Minderhoud, M. 1999. Supported Driving: Impacts on Motorway Traffic Flow. PhD thesis, Delft University of Technology.

NAGEL, K. 2004. A cellular automaton model for freeway traffic. Journal de Physique.

Ni, D., 2015. Traffic Flow Theory: Characteristics, Experimental Methods, and Numerical Techniques. Butterworth-Heinemann ISBN: 9780128041345.

Park, D., You, S., Rho, J., Cho, H. Lee, K. 2007. Investigating optimal aggregation interval sizes of loop detector data for freeway travel-time estimation and prediction. NRC Research Press, Department of Transportation Engineering, University of Seoul.

Struijs, P. 2014. Traffic loop data for transport statistics. International Conference on Big Data for Official Statistics. Beijing, China.

Sugiyama, Y., Fukui, M., Kikuchi, M., Hasebe, K., Nakayama, A., Nishinari, K., Tadaki, S.I. and Yukawa, S., 2008. Traffic jams without bottlenecks-experimental evidence for the physical mechanism of the formation of a jam. IOP Publishing and Deutsche Physikalische Gesellschaft. Department of Complex Systems Science, Nagoya University, Japan.

TRB, 2000. Highway Capacity Manual. Transport Research Board, National Research Counsil Washington D.C. USA.

Vonk Noordegraaf, J. van Huis, J. Baan, T. Vonk, T. Bakri, and P. van den Haak 2013. Filegolven Rotterdam, TNO. FHWA, Localized Bottleneck Reduction Program.

Wang, H., Li, J., Chen, Q.Y., Ni, D. 2009. Speed-Density Relation: From Deterministic to Stochastic. Resubmitted to TRB 88th Annual Meeting at Washington D. C.

Weg, G.S. van, Hegyi, A 2014. Resolving moving jams on the A13 Development and evaluation of extensions of COSCAL v2 G.S. Delft University of technology.

Wilensky, U., 1999. Netlogo. Center for Connected Learning and Computer-Based Modelling. http://ccl.northwestern.edu/netlogo/.

Wu, N., A new approach for modelling of Fundamental Diagrams. Transportation Research Part A: Policy and Practice, Vol. 36, No. 10, 2002, pp. 867–884, doi: DOI: 10.1016/S0965- 8564(01)00043-X.

Yuan, Y., van Lint, J.W.C., Schreiter, T., Vranken, J.L.M., 2010. Automatic speed-bias correction with flow-density relations. Conference: Proceedings of the IEEE International Conference on Networking, Sensing and Control. Chicago, IL, USA.

Yuan, K., Knoop, V.L., Hoogendoorns, S.P., 2014. CAPACITY DROP: A RELATION BETWEEN THE SPEED IN CONGESTION AND THE QUEUE DISCHARGE RATE. Department of Transport and Planning Faculty of Civil Engineering and Geosciences Delft University of Technology.